DOE FINAL TECHNICAL REPORT

U.S. Department of Energy Grant No. DE-SC0012551

Visualization of Multi-Dimensional Imaging Data for the DIII-D National Fusion Facility

April 30, 2018

PRINCIPAL INVESTIGATOR:

Prof. N.C. Luhmann, Jr.

Phone: (530) 752-5414

Facsimile: (530) 754-9070

Email: ncluhmann@ucdavis.edu

UNIVERSITY OF CALIFORNIA, DAVIS

Department of Electrical and Computer Engineering

EXECUTIVE SUMMARY

With funding provided from the Office of Fusion Energy Science's program on Diagnostic Systems for Magnetic Fusion Energy Sciences, the PI and his team have pioneered the development of microwave imaging systems for magnetic fusion plasma diagnostics. Specifically, electron cyclotron emission (ECE) imaging [1], a passive radiometric technique, measures electron temperature fluctuations; and microwave imaging reflectometry (MIR) [2], an active radar imaging technique, measures electron density fluctuations. These microwave imaging diagnostic instruments developed by UC Davis have made important contributions to fusion science in a relatively short period of time from their original installation on DIII-D. The microwave imaging diagnostic technique has matured considerably since the beginning of a fruitful collaboration with DIII-D and PPPL, and has also been adopted at preeminent tokamak facilities worldwide. As discussed in detail in the following, this has continued with the development of revolutionary microwave diagnostic instruments employing monolithic millimeter wave integrated circuit (MMIC) system-on-chip (SoC) technology. Specifically, "chip" receivers mounted in liquid crystal polymer (LCP) modules have been demonstrated to dramatically improve the performance of the electron cyclotron emission imaging (ECEI) system including: 30x improvement in noise temperature thereby permitting absolute 2-D electron temperature images, outstanding shielding against out-of-band interference including microwave bursting which had plagued previous ELM studies using the old quasi-optical mini-lens ECEI system, and independent modules facilitating flexible repair and replacement.

Under the "Visualization of multi-dimensional imaging data for the DIII-D National Fusion Facility" program, funding was provided for a research scientist postdoc and a Ph.D. student to support physics studies at DIII-D employing these instruments. This endeavor is synergistic with our current grant under the DOE Fusion Energy Sciences (FES) program on Diagnostic Systems for Magnetic Fusion Energy Sciences. This support considerably increased the scientific output of the diagnostics. The activities were strongly focused in the areas of **pedestal and ELM stability**, **energetic particle confinement**, and the **early detection and avoidance of tokamak disruptions** employing the microwave imaging diagnostic instruments developed under the advanced diagnostics program where imaging of the ELM crash was made possible by the elimination of the interference from the associated microwave "bursts"

1. BACKGROUND AND INTRODUCTION

Conventional electron cyclotron emission (ECE) radiometry employs a single wideband receiver to resolve multi-frequency ECE into a spatially varying temperature profile, and has been a standard diagnostic for magnetic fusion plasmas for over thirty years. Such systems, however, are limited to 1-D horizontal measurements along the major radius and often feature a relatively poor poloidal spatial resolution. The PI pioneered the approach of optically imaging the emission onto a vertically aligned array of detectors, which expands the capabilities of ECE radiometry to two dimensions and is referred to as ECE-Imaging and is illustrated in Fig. 1.

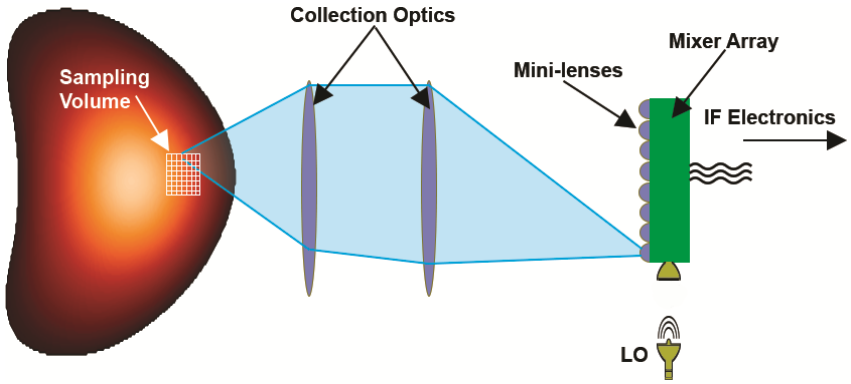

Fig.1. Schematic illustration of the principles governing ECEI.

The value of 2-D ECE-Imaging for T_e fluctuation imaging and physics studies was first demonstrated on the TEXTOR tokamak in a UCD/PPPL/FOM collaboration. Significant advances over this first proof-of-principle instrument were made, beginning with an advanced instrument installed on TEXTOR that provided 16×8 image resolution. This TEXTOR system was subsequently transferred to ASDEX-Upgrade where it began collecting data in June, 2009. A new imaging array arrangement with enhanced optical performance and increased sensitivity was then developed by UCD and PPPL for DIII-D which began collecting data in March of 2010 and demonstrating the full capability of this technique to unravel crucial physics questions.

The PI's group has also pioneered the development of microwave imaging reflectometry (MIR) instruments that permit one to obtain spatially resolved "pictures" of the fusion plasma density fluctuations and have implemented systems on major fusion devices such as the DIII-D tokamak. Reflectometry provides a localized measurement, relying on the reflection of a microwave beam from the cutoff surface; when properly coupled, the reflected beam is phase-modulated by fluctuations of the index of refraction near the cutoff surface making it possible to provide an image of the turbulent fluctuations. However, in the presence of 2D fluctuations (i.e. where there are fluctuations in both the poloidal and radial directions), it is difficult to provide a clear interpretation for conventional reflectometry data. The difficulty arises from the fact that when the plasma permittivity fluctuates perpendicular to the direction of propagation of the probing wave, the spectral components of the reflected field scatter into a large solid angle resulting in fragmented wave fronts with a complicated pattern of amplitude and phase fluctuations. The solution (originally conceived by collaborator Ernesto Mazzucato) is to employ imaging techniques whereby the illumination beam is transformed into an extended beam whose curved wave front is designed to roughly match the poloidal shape of the plasma cutoff layer. The wave front curvature matching thereby projects a nearly constant phase front onto the fluctuating layer. The reflected beam passes through additional optics utilized to image the reflecting layer onto the detector array, as illustrated in Fig. 2, and the resultant detector signal is nearly purely phase modulated. Probing the plasma simultaneously with multiple frequencies produces a 2D image of turbulence and magnetohydrodynamic (MHD) eigenmodes. It allows for analysis of radial and poloidal correlation lengths, wavenumbers, and both the phase and group velocity of propagating modes.

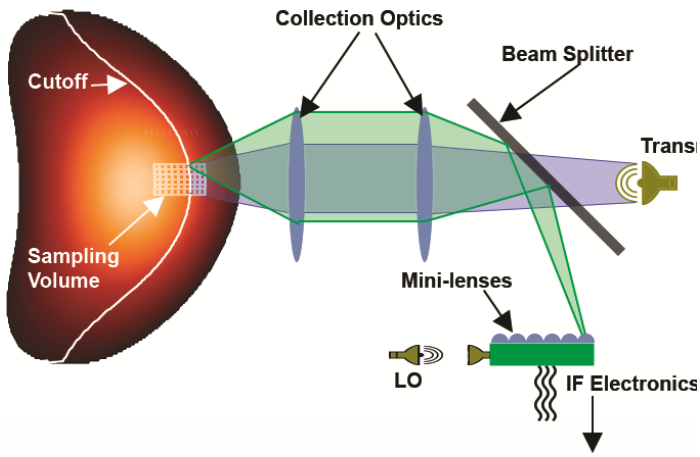

Fig. 2. Schematic illustration of the principles governing MIR.

The MIR technique was demonstrated by UCD and PPPL with a proof-of-principle instrument installed on the TEXTOR tokamak. This provided confidence in the development of an advanced 2-D MIR system which was installed on DIII-D in May 2013 and began taking plasma data in July 2013. The instrument is designed to take full advantage of the large aperture port it shares with the ECE Imaging diagnostic to access large regions of the DIII-D plasma. A broad frequency range (56 – 74 GHz) and 12-element antenna array map to a poloidal cross-section of the plasma.

Under continued OFES diagnostic development funding, UCD has developed revolutionary microwave diagnostic instruments employing monolithic millimeter wave integrated circuit (MMIC) system-on-chip (SoC) technology which facilitated physics studies conducted under the "Visualization of multi-dimensional imaging data for the DIII-D National Fusion Facility" program. Specifically, "chip" receivers mounted in liquid crystal polymer (LCP) modules have been demonstrated to dramatically improve the performance of the electron cyclotron emission imaging (ECEI) system including: 30x improvement in noise temperature thereby permitting absolute 2-D electron temperature images, outstanding shielding against out-of-band interference including microwave bursting which had plagued previous ELM studies using the old quasi-optical mini-lens ECEI system, and independent modules facilitating flexible repair and replacement. A proof-of-principle test of a full system (20 poloidal channels) utilizing commercial E-band receiver chips (intended for point-to-point wireless communications) was installed in February 2018, as shown in Figure 3. Although these were limited from 72 to 81 GHz (instead of the full 60 – 90 GHz of E-band), they were suitable for the DIII-D pedestal region ELM imaging measurements during operation under toroidal magnetic fields from 1.7 to 1.8 T.

The capability of the LCP ECEI system to provide absolute electron temperature measurements and profiles is demonstrated in Figure 4. Here, it was calibrated against the Thomson scattering diagnostic since access was not available to insert our extended black body source inside the vessel which will provide a fully stand-alone calibration. The two-dimensional absolute electron temperature profile has been captured during inter-ELMs, which is very helpful to monitor the temperature profile crash and recovery for ELM dynamics investigations.

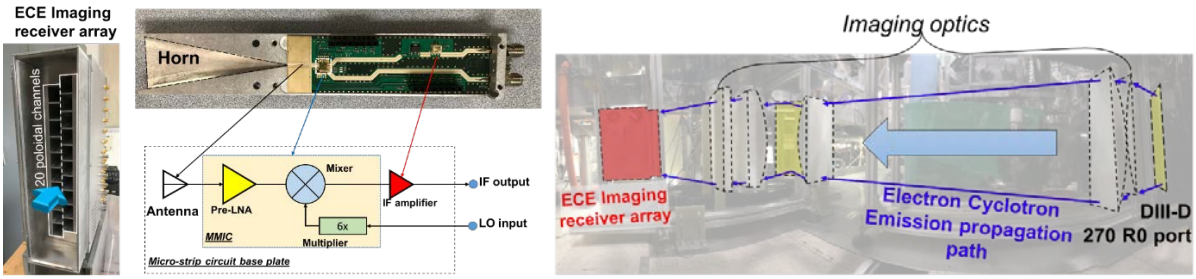

(a) (b)

Figure 3. (a) There are 20 poloidal channels in the ECE Imaging receiver array. Each receiver chip is mounted on microstrip circuit substrate with individual shielding housing. (b) ECE Imaging had been successfully installed at 270 R0 port on DIII-D for 2D electron temperature profile and fluctuation imaging measurement.

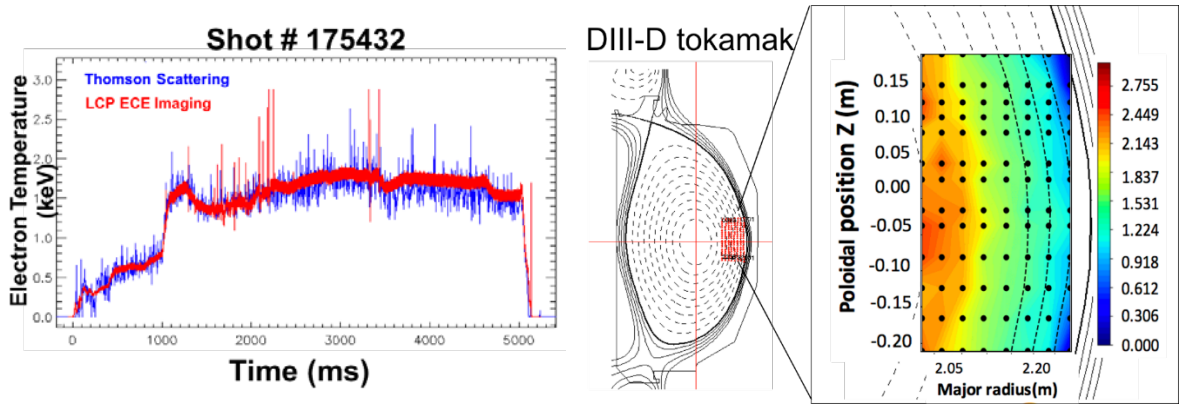

(a) (b)

Figure 4. (a) The blue curve shows the electron temperature measured by Thomson scattering. The red curve shows the calibrated temperature by ECE Imaging. (b) The 2D temperature profile for 1774.14 ms during shot 175432.

The SoC technology is also being employed for the microwave imaging reflectometer (MIR) system. The DIII-D MIR instrument developed and installed in 2013 uses a 12-vertical-channel Schottky diode heterodyne receiver array with 4 simultaneously tunable transmitter signals, thus providing a 12x4 pixel image. On the receiver side, the existing system includes 12 vertically-aligned elements with a mini lens attached to each element to receive RF and LO signals following which then the down-converting process occurs in the first stage. Here, there exists a critical problem preventing all of the elements from performing identical behavior such as conversion gain. The LO drive power for each antenna is slightly different because the quasi-optical coupling can result in alignment issues and non-uniform beam pattern causing a variation in conversion gain over the array which requires further attenuated calibration. In addition, the Schottky diode heterodyne receiver possesses high noise and large conversion loss in the front-end with resulting system noise temperature of ~55,000 K.

The original MIR transmitter architecture is built up with commercially available waveguide components resulting in a large and bulky configuration. Low frequency microwave sources are up-converted to V-band (55-75 GHz) using an up-converting mixer. The RF output of the mixer is then amplified and radiated from a standard horn antenna. However, the main challenge here is the limited number of tones due to the maximum available output power of the V-band power amplifier. This meant that for the EHO studies described below, there were only 2 radial channels of interest.

Aimed at increasing the spacing resolution and bandwidth of the current system, the CMOS-based transmitter expands the capabilities to illuminate 8 separate frequencies simultaneously located within V band (55-75 GHz). In other words, the output frequencies are tunable over the entire 20 GHz bandwidth covering the wide dynamic range for the DIII-D tokamak. Figure 5 shows the chip photo presenting four low frequencies IF inputs, V-band LO input, and RF output port. The output spectrum of the transmitter with 64 GHz LO input illustrates eight tones with around 0 dBm power level.

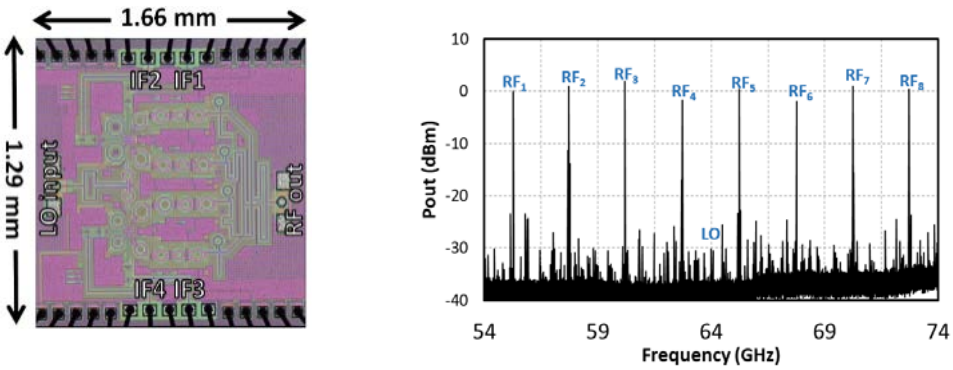

Figure 5. Photo and measured output spectrum of V-band MIR transmitter

On the receiver side, the existing MIR system includes 12 vertically-aligned elements with a mini lens attached to each element to receive RF and LO signals following which then the down-converting process occurs in the first stage. Here, there exists a critical problem preventing all of the elements from performing identical behavior such as conversion gain. The LO drive power for each antenna is slightly different because the quasi-optical coupling can result in alignment issues and non-uniform beam pattern causing a variation in conversion gain over the array which requires further attenuated calibration. In addition, the Schottky diode heterodyne receiver possesses high noise and large conversion loss in the front-end with resulting system noise temperature of $\sim$55,000 K. Figure 6 presents the architecture of the V-band receiver chip. A compact, low-noise, and easy-assembling in-house design receiver chip includes a three-stage broadband low-noise amplifier, a double-balanced mixer, and an IF amplifier offering more accurate sensing capability. The V-band receiver for the MIR system upgrade has been designed, fabricated, and tested. Aimed at improving the noise temperature and overall conversion gain through the entire 20 GHz bandwidth, the CMOS-based receiver is measured to offer about 30 dB conversion gain with noise figure lower than 10 dB (noise temperature below 2,600 K). In addition, the LO drive is fed directly from waveguide thus preventing misalignment.

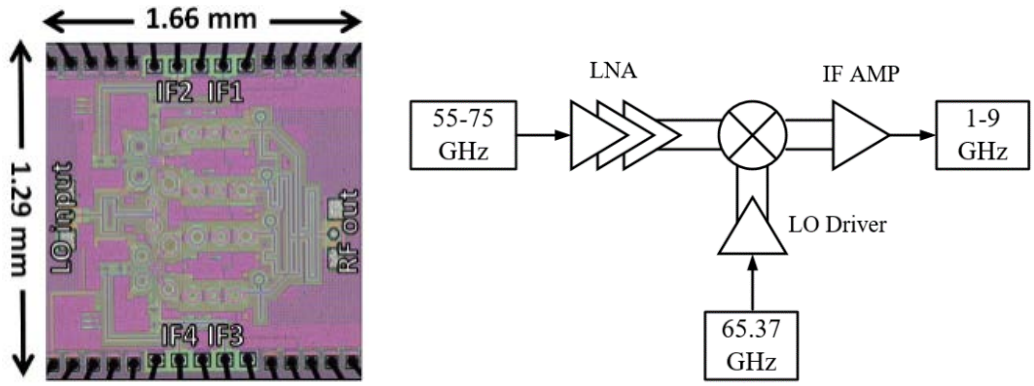

Figure 6. V-band receiver chip photo and architecture

It is noteworthy that this imaging endeavor (both technology development and physics studies) has been primarily a student-led development over successive generations of DoE support resulting in domestic/international proof-of-principle systems. Specifically, all of the instruments have been designed and fabricated at UC Davis with the physics studies carried out in longstanding collaborations between UC Davis, Princeton Plasma Physics Laboratory (PPPL), POSTECH University (Pohang, South Korea), the University of Science and Technology (USTC) in Hefei, China, and the University of Colorado.

The supportive environment offered by the DIII-D research community has been key to the education of young researchers from UC Davis during the development of ECEI and MIR diagnostics there. During the period since these diagnostic capabilities were first delivered to the DIII-D facility, graduate students have been active participants in groundbreaking research conducted in important areas such as energetic particle confinement, tearing stability, and edge localized modes, and drift wave turbulence, among many others. The philosophy behind the establishment of a postdoctoral research position has been to facilitate the greater dissemination of imaging diagnostic data while providing reliable on-site support for the ambitions of now 12 current and former graduate students who have made DIII-D physics research an integral part of their graduate dissertation research. Added to this are another 3 summer undergraduate students that studied at DIII-D, plus 12 graduate students whose dissertations are focused on technological advances that support UC Davis plasma diagnostic instruments. Their work has produced 32 student-led, peer-reviewed journal publications and conference proceedings.

2. RECENT DEVELOPMENTS AND ACCOMPLISHMENTS

1-Microwave imaging diagnostics

The ECEI system originally installed on DIII-D (and still available for experiments) was virtually a mirror image of the diagnostics that UC Davis designed and delivered to KSTAR and AUG [G.S. Yun et al., Phys. Rev. Lett. 107, 045004 (2011); J. Lee et al., Phys. Rev. Lett. 117, 075001 (2016). There has always been great enthusiasm about our imaging results there, and optimism that this success could be repeated at DIII-D where discharges are generally either better diagnosed or attaining dimensionless parameters closer to those expected on ITER. However, there appears to be something fundamentally

different about the DIII-D edge plasma. We attribute this difference to the properties of plasmas at lower collisionality. During the most interesting discharges, and particularly in the highly nonlinear phases of each ELM, intense bursting occurs across a broad range of microwave frequencies [B. J. Tobias, et al., EPS 2012, Stockholm, 2012, L. Yu, et al., APS DPP, 2013, Fuchs and M. E. Austin, Phys. Plasmas, vol. 8, no. 5, 2001.]. Some of these bursts are so intense that they actually burn out otherwise very robust diagnostics [G. Hanson, private communication]. Without properly shielding against and rejecting out-of-band microwave emission, the diagnostic data are of poor quality and of little use for the most interesting physics studies. This prompted a change of course within our diagnostic development program that we are happy to say has resulted in dramatically improved instrumentation with greater prospects for application in the even more demanding operating environments that will come with the ITER era.

ECE-Imaging has been transformed on DIII-D with new technologies that place the entire down-converting receiver, including the previously bulky LO chain, on a single microchip ("System-on-Chip-SoC) that is completely shielded from interference and stray radiation inside a compact, metallic enclosure [Yan Wang, et al, NF, 57:7, 072007 (2017)]. This dramatically reduces size, power consumption, and cost, but more importantly provides reliable performance and enhanced capability. ECEI can now be calibrated for absolute 2D temperature profile measurement, system noise temperature is improved by orders of magnitude, and out-of-band interference from ECH and microwave bursting (the latter of which has frustrated attempts to image ELMs on DIII-D) is eliminated [Yilun Zhu, "Status of the ECE Imaging Upgrade for ELM Imaging", presented at DIII-D Friday Science Meeting, June 23, 2017]. Figure 7 shows an example of test data taken early on during commissioning of a new ECEI receiver. Note that there is no interference on the ECEI channel shown, even while injecting more than 3 MW of ECH power. This level of rejection was not possible with the previous system, even with -60 dB notch filters in place.

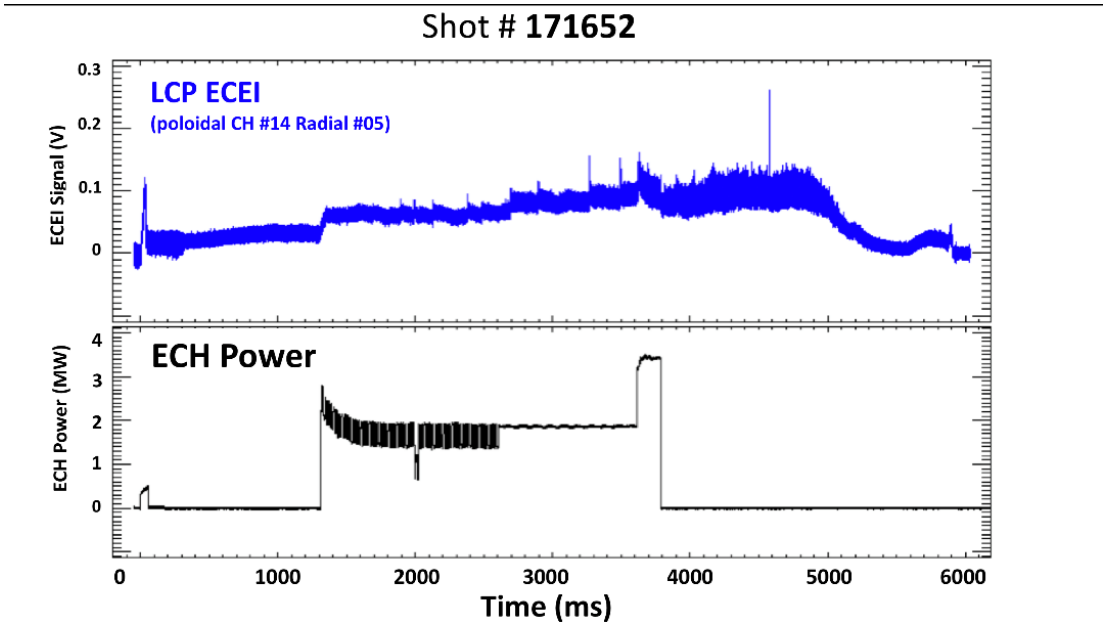

Figure 7. Signals from the upgraded ECEI system showing no anomalous interference from ECH power, even at levels greater than 3 MW.

In Figure 8, the impact of improved circuit shielding on spurious bursts of out-of-band microwave emission is shown. The black trace is data obtained by the original mini-lens imaging array. The red data is from the new LCP design, same shot, same measurement frequency. The two arrays were operated side-

by-side for direct comparison, and none of the spurious signals that would obscure temperature measurements at the beginning or end of the discharge pose a problem for the new system.

Not every burst or spike appearing on ECEI data is removed by improvements in shielding and interference rejection. This is important, however, because some bursting is actually within the acceptance bandwidth of the diagnostic channel. These signals can now be imaged and properly interpreted for the purpose of better understanding of the nature of the bursting itself. Take, for example, the data shown in Figure 9. The original ECEI system recorded the black trace, almost completely saturated by interference for 200 microseconds, the entire duration of the nonlinear ELM phase. The new diagnostic shows that only a single isolated spike at 1815.8 ms is actually within the diagnostic bandwidth. The rest of the bursts are rejected, while that remaining burst can be properly characterized and studied for its physical relevance.

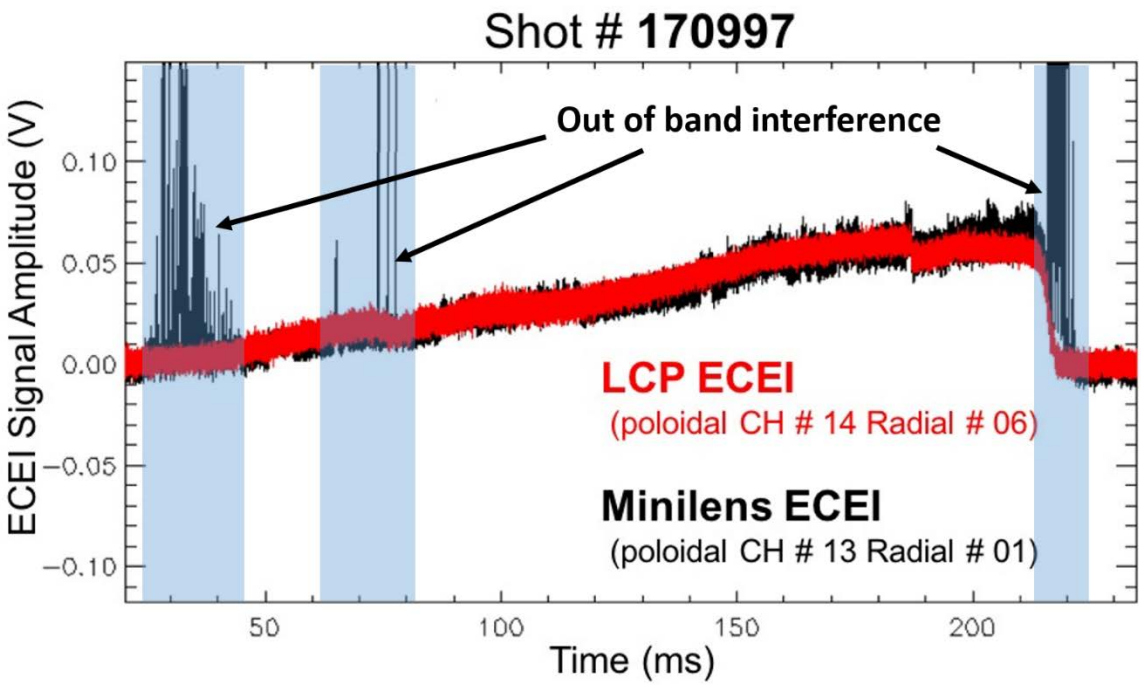

Figure 8. Data from both the old (mini-lens) and new (LCP) ECEI systems on DIII-D. Data is obtained during the same discharge and at the same frequency, viewing the same region of the plasma. The new system is clearly far less impacted by spurious interference from out-of-band RF bursting radiation.

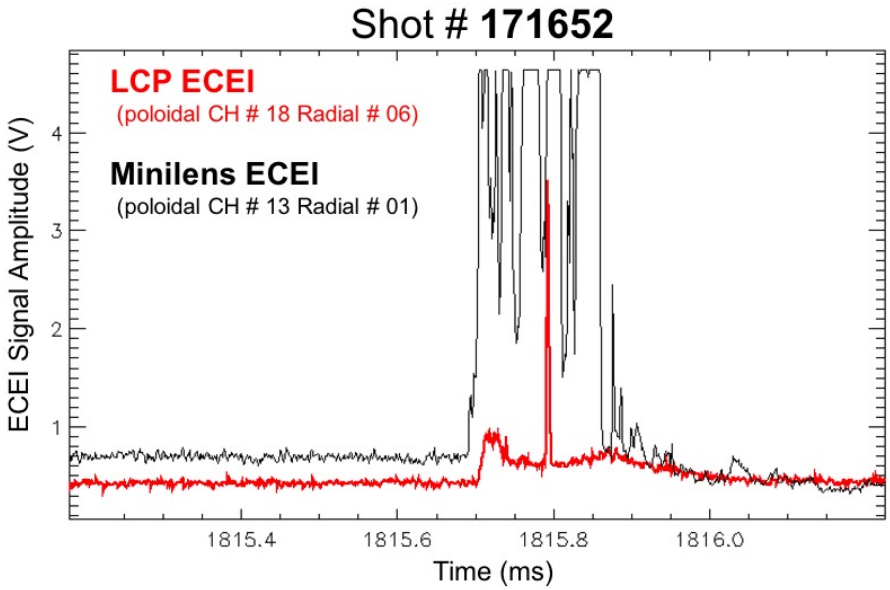

Figure 9. A comparison of old and new systems when applied to ELM imaging. Nearly all the transient spikes in temperature observed by the old system are eliminated. Those that remain are in-band and may be characterized for physics understanding.

During the end of the FY17 DIII-D run period, the initial embodiment of this new system was installed on DIII-D and shown to 1) exhibit improved rejection of interference from transient plasma radiation (compared to the previous ECEI system as well as the ECE system) and 2) maintain a stable calibration for absolute temperature measurement (other ECEI diagnostics only measure relative, or fluctuating T_e).

Though only a limited number of complete modules (8 versus the total 20 that will be deployed in a full-scale system following the LVO) were available as prototypes at the time of testing, making for small images with limited range and resolution, successful imaging of core modes demonstrates that the new approach has merit and there are no outstanding barriers to a full-scale upgrade. Figure 10 shows sample images of Alfvén eigenmodes obtained with the new system. Only 6x8=48 channels were used (versus the 160 that will be available after the LTO), but the diagnosed mode structure is consistent with extensive studies carried out in years past.

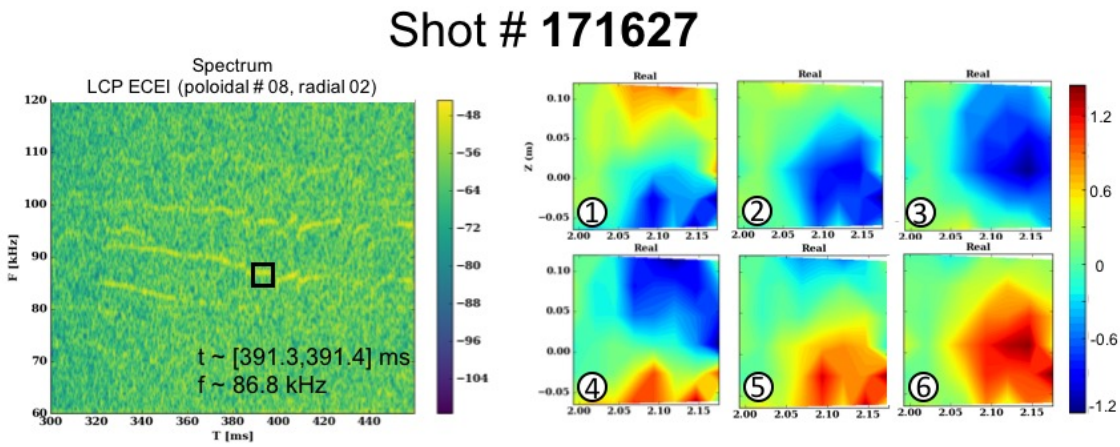

Figure 10. Spectra and 2D images of Alfvén eigenmodes obtained with a limited number of channels from the prototype ECEI upgrade.

As illustrated in Fig. 11, there will be two more major upgrades which will extend the frequency coverage (75- 140 GHz) and the depth of focus (10 cm to 100 cm) enabling ELM studies over a wide range of ITER relevant DIII-D operating conditions.

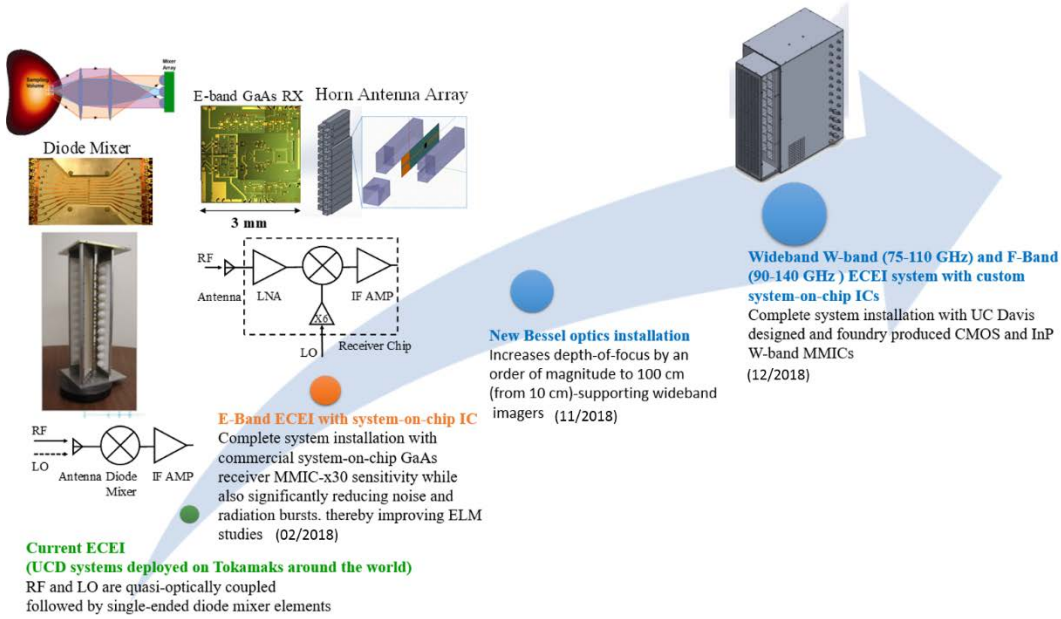

Figure 11. The development roadmap for ECEI diagnostics.

Much has been said so far about ECEI and the successful application of ECEI for ELM physics studies. However, it is equally important to recognize the role that MIR plays in providing data for these studies. MIR has already proven valuable in our EHO studies on DIII-D. Figure 12 provides an example of EHO investigation with collaborative measurement of beam emission spectroscopy (BES) and MIR. As complementary density fluctuation diagnostics, they both provide details of the mode structure. In this case, the radial wavenumber was obtained by BES while the poloidal mode number was inferred from MIR data. For many applications, they provide independent corroborating measurements. This cross checking

becomes important when neutral beam timing or other experimental needs prevent BES data from being collected.

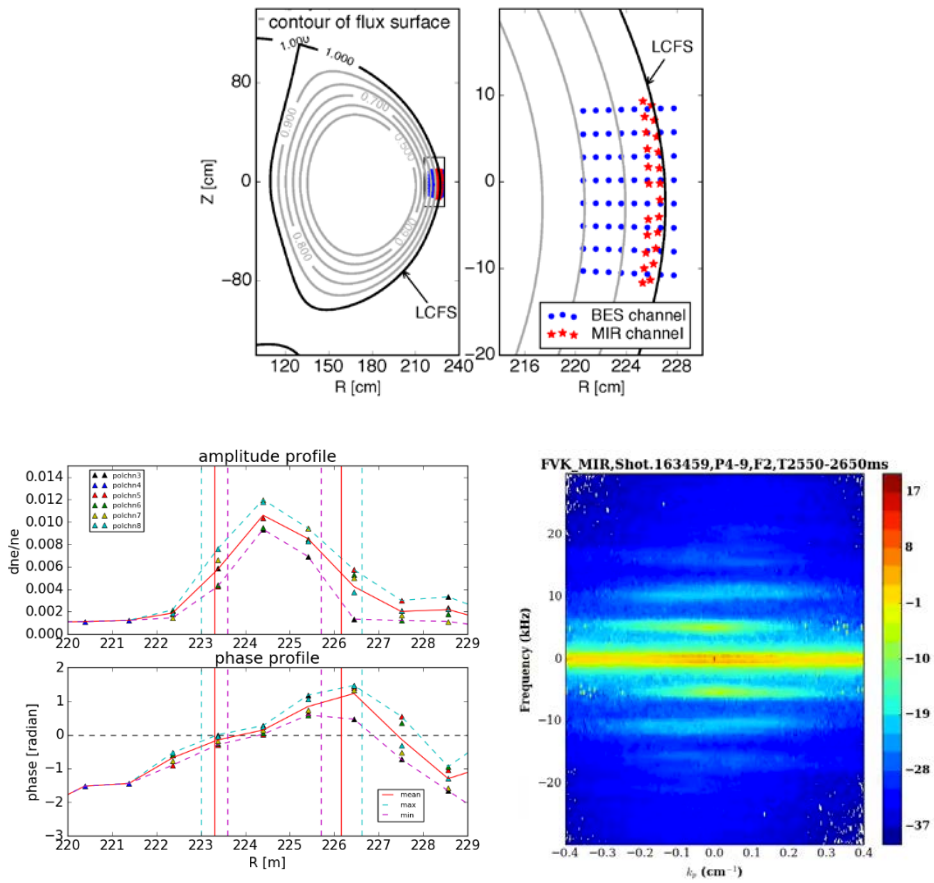

Figure 12. The top figure shows the collaborative measurement region of BES and MIR.The mode structure (mode amplitude and phase versus radius) obtained from BES data shown at bottom left. At bottom right, the poloidal wavenumber spectrum as a function of frequency obtained from MIR data.

The occurrence of ELMs, transient instabilities of the H-mode pedestal resulting in elevated heat and particles fluxes to the vessel wall, poses a significant challenge to ITER. DIII-D has been a world leader in ELM suppression and mitigation, perhaps most notably in the development of ELM suppression techniques using resonant magnetic perturbation (RMP). Imposing 3D fields on the plasma with external magnetic coils has successfully eliminated ELMs in many cases, and there is great motivation to develop these techniques further, demonstrating their compatibility with various ITER operating scenarios and in particular overcoming the challenges of simultaneously maintaining fusion performance in the core plasma. In parallel with this work, DIII-D researchers have discovered new operating regimes in which quiescent transport barriers are able to improve confinement without triggering transient events. Here, we refer to the so-called QH-mode, where a saturated coherent edge fluctuation replaces the fast-growing peeling-ballooning instability that leads to an ELM. Although initially confined to regimes of low density and significant counter-current rotation, considerable progress has been made in expanding the QH- mode regime to more fusion relevant parameters. The most recent results from DIII-D suggest that the rotational shear required to modify pedestal stability can, in fact, be maintained in the pedestal region with low levels of injected torque, an important milestone for demonstrating ITER compatibility. Furthermore, a new regime of pedestal stability has been identified, in which a broadband fluctuation replaces the so-

called coherent Edge Harmonic Oscillations (EHOs). These discharges develop a tall, wide density pedestal of the kind necessary to improve fusion performance in the core.

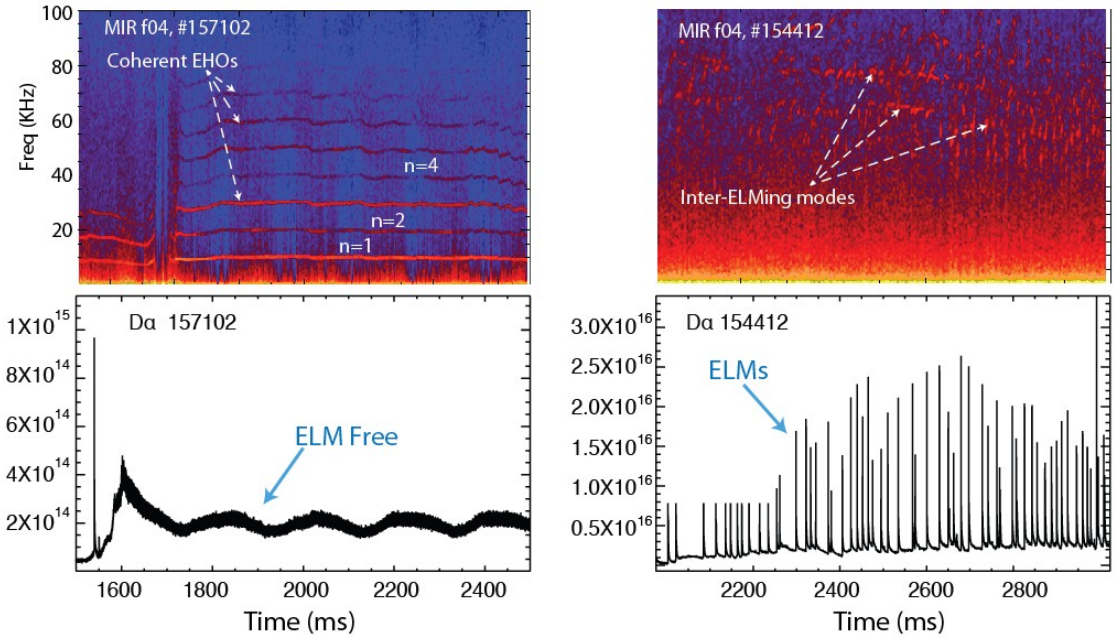

Figure 13. Density fluctuation spectra of an edge harmonic density oscillation with dominant n=1, 3 components diagnosed by MIR (upper left). The corresponding divertor light obtained by filterscopes (bottom left) with slow modulation produced by sweeping the plasma edge. MIR spectra during normal ELMing H-mode, with higher frequency inter-ELM modes (upper right). Spikes of Dα emission during the same time (bottom right).

Employing the microwave imaging diagnostics, UC Davis has been a key contributor to investigation of the so-called broadband edge harmonic fluctuation, or broadband MHD on DIII-D. This mode has been the subject of Microwave Imaging Reflectometry (MIR) and a notably successful application of this diagnostic. Chris Muscatello, then a UC Davis postdoctoral researcher, demonstrated scientific leadership in recognizing the significance of data collected during the early commissioning phases of the MIR diagnostic on DIII-D (see Fig. 13). Using the localized, 2D density fluctuation data available from MIR, he succeeded in demonstrating that broadband fluctuations observed in these new QH-mode regimes propagated independently from the coherent EHOs that characterize other QH-mode discharges (see Fig. 14). This observation illustrates unambiguously that the broadband EHO is, in fact, a different instability, driven unstable by different mechanisms and therefore necessitating a very different control strategy for optimizing the performance of discharges in which it dominates.

Since Chris Muscatello's important observations, UC Davis graduate students Xiaoxin Ren and Ming Chen worked to validate the data and work with DIII-D researchers to understand its significance. This work is performed by comparing ECE-Imaging and MIR data with plasma simulations. Of course, the complexity of microwave imaging data makes the direct interpretation of images produced problematic. This is true of all diagnostic techniques, but special challenges complicate the direct interpretation of pedestal images produced by microwave radiometry and reflectometry. The correct method of comparing diagnostic data with plasma simulation is to accurately model the response of the diagnostic system to a proposed model of the plasma behavior. This is referred to as synthetic diagnostic forward modeling and described in the next section.

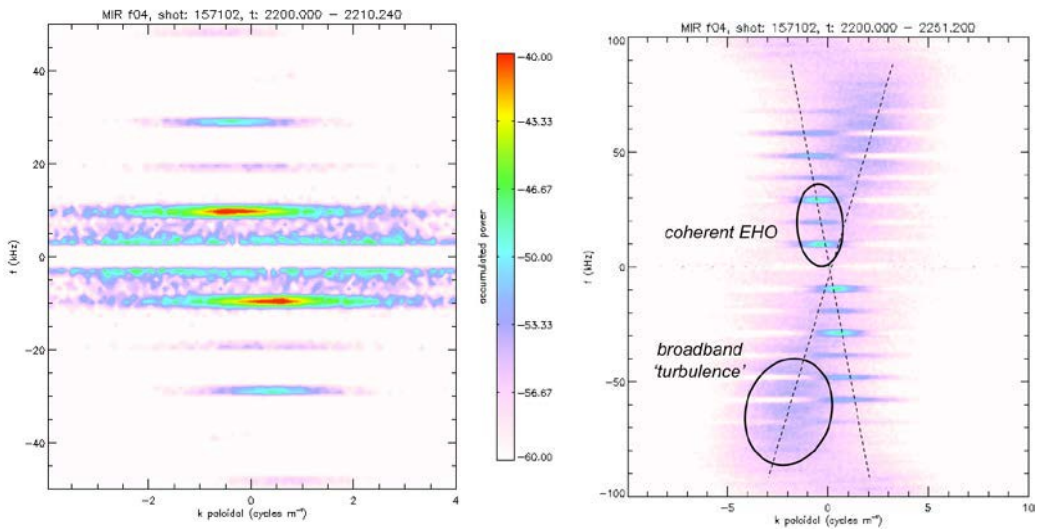

Figure 14. The 2D power spectral density obtained by MIR during QH-mode on DIII-D. Coherent EHO (left) has dominant n=1 and n=3 harmonics. At times when both the coherent EHO and a broadband feature can be distinguished (right), their fluctuations propagate poloidal in different directions.

Under this program, Ming Chen, a former UC Davis Ph.D. student, carried out detailed observations of the EHO observed in QH-mode discharges at DIII-D. One important aspect of this mode is the edge radial electric field. Considerable theoretical work done on peeling-ballooning instabilities and other edge-localized fluctuations suggests a connection between edge toroidal flow shear and the linearly unstable spectrum (more will be said on this in later sections). A corollary implication for the EHO is the question as to whether or not there may be a so-called critical E×B shear for exciting the EHO or transitioning into any related ELM-free state. It is therefore interesting to explore the relationship between E×B shear and mode structure. In Figure 15 below, the E×B shearing rate is evaluated for two types of QH-mode discharges, both exhibiting an EHO. Nearly a two-fold variation of shearing rate is possible while maintaining a saturated EHO.

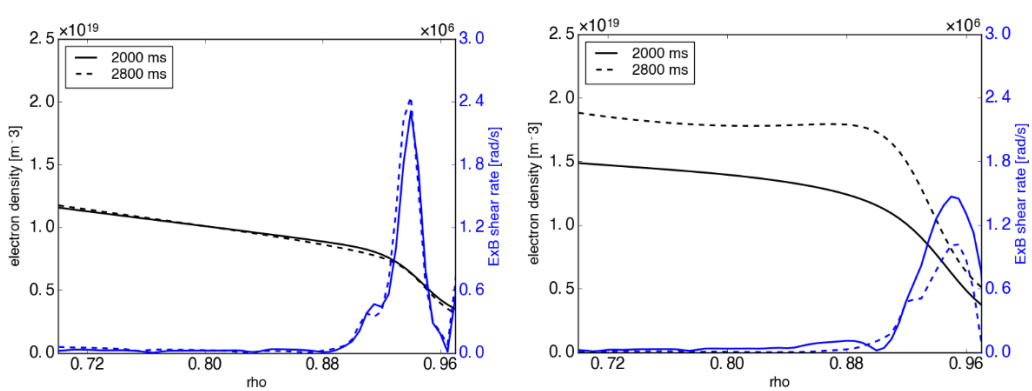

Figure 15. The fitted E×B shearing rate is shown for discharges with constant injected torque (left) and with torque reduced over time (right).

In Figure 16a, the poloidal wavenumber spectrum of the EHO, as measured by microwave imaging reflectometry (MIR), is shown. Though the mode is heavily damped, a natural consequence of being strongly driven (evident from the impact on pedestal profiles) and persisting in a saturated state, it is clearly

shifted to an identifiable central wavenumber that corresponds to the toroidal mode number. In Figure 16b, it is clear that this poloidal wavenumber spectrum does not change with E×B shear. However, another important trend does arise: the radial wavenumber, a measure of the shearing or twisting of the mode structure, increases with increasing E×B shear rate. This quantitative result will be valuable in comparison with plasma simulation—it has a direct impact on power balance and nonlinear stability and provide consistent explanation for the improved confinement. This work had been presented at the 1st Asia-Pacific Conference on Plasma Physic at Chengdu, China, where Ming Chen gave a contributed talk.

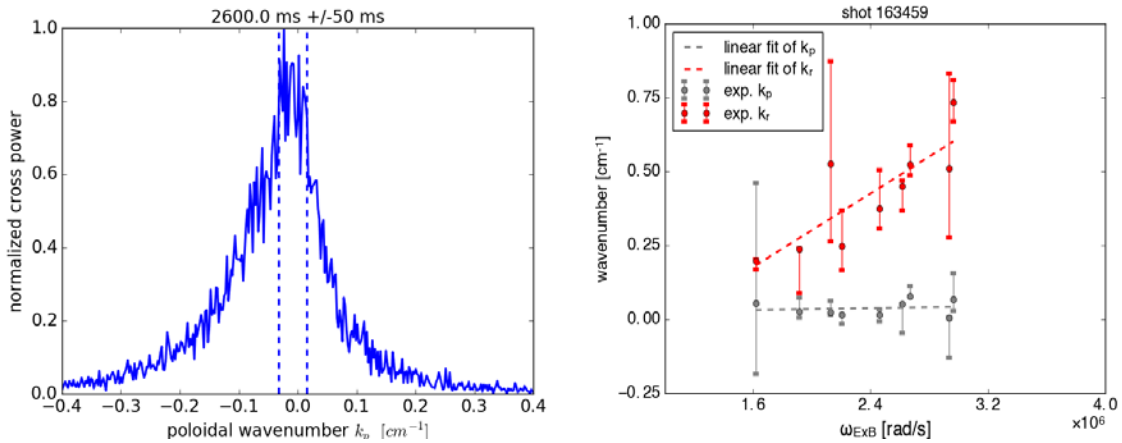

Figure 16. The measured poloidal wavenumber of an EHO as obtained by MIR imaging (left), and variation both the poloidal and radial wavenumber as a function of varying E×B shearing rate.

As with ECEI, there is an ambitious near-term development path laid out for MIR. Major upgrades in the form of custom MMICs and SOC designs are already in the works and will be made available at DIII-D in the coming year. *Again, these diagnostic developments are independently funded by the diagnostics development program.*

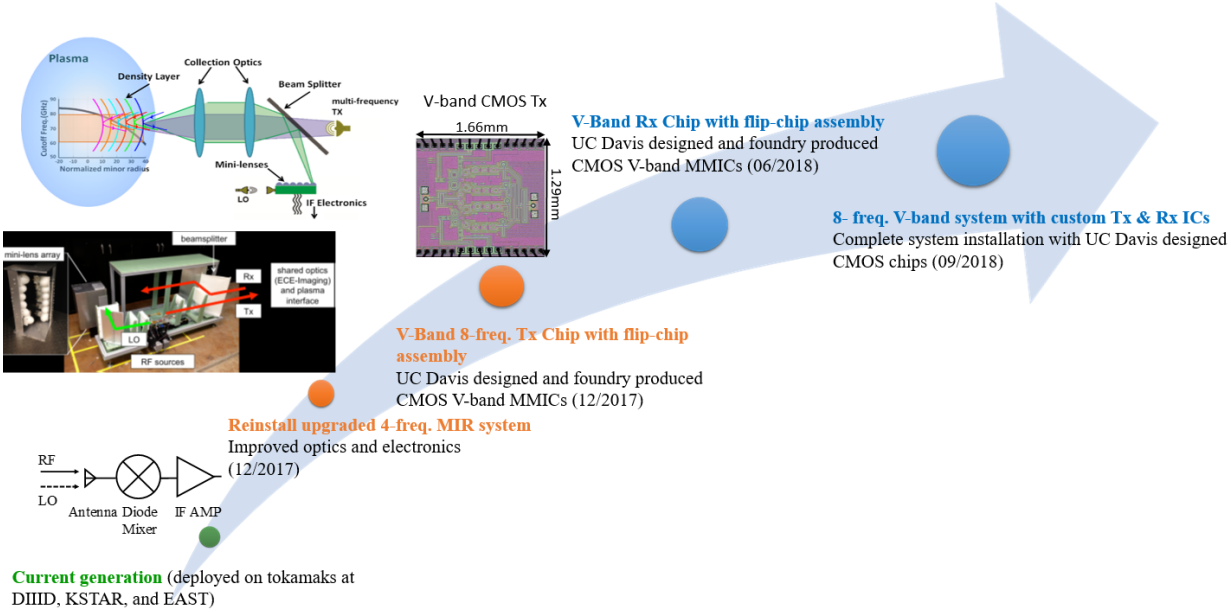

Figure 17. The development roadmap for MIR diagnostics.

2-Synthetic diagnostics and data visualization

Our view is that quantitative inference from data analysis depends upon the comparison of carefully processed experimental data with synthetic diagnostic forward modeling. The direct interpretation of data is fraught with pitfalls, particularly with sophisticated instrumentation and complex physical processes in the plasma serving to generate microwave signals. Generally, this approach only works when applied by the most experienced and expert diagnosticians, and only under very limited circumstances when the most helpful approximations hold. It is of little utility in exploratory science, when the phenomena of interest are unfamiliar or the underlying conditions are not well-known. The preferred approach is statistical inference, i.e. the application of a rigorous probabilistic methodology such as Bayesian maximum a posteriori analysis. While a comprehensive approach to iterative likelihood optimization is not yet within the reach of the microwave imaging community, we have made great strides in synthetic diagnostics for ECEI and MIR. This section describes progress in this challenging, but important, first step toward routine and automated quantitative inference while detailing the important role it plays in the validation of plasma simulations.

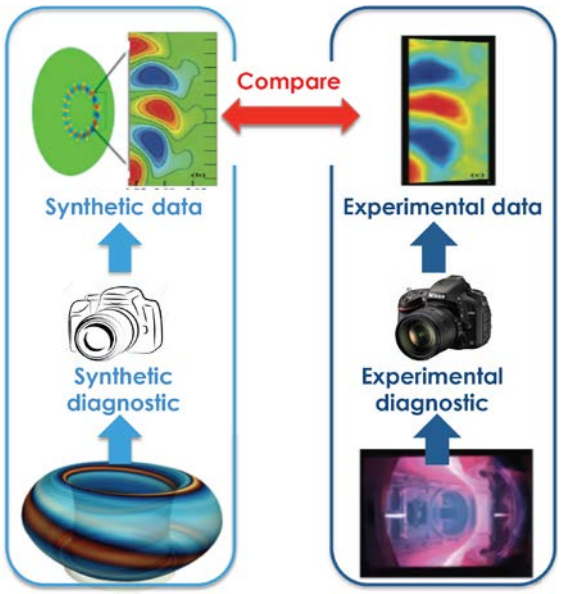

Figure 18. Data analysis through comparison with forward modeling.

Partnerships with PPPL (Ernie Valeo, Gerrit Kramer), and Lei Shi (former post-doctorate researcher at the University of California Irvine with Z. Lin and former graduate student at Princeton University) under the Innovative Diagnostics Program have provided a sophisticated platform for coupling a wide variety of MHD and gyrokinetic codes with models for the diagnostic response and comparing them with real data [(X. Ren, et al., J. Inst. 2015, Shi, et al., RSI, 87, 11D303 (2016); E. J. Valeo et al., Plasma Phys. Control. Fusion 44 (2002) L1–L10]. Through these collaborations, we intend to integrate this capability with other analysis tools within the open-source OMFIT environment at DIII-D, facilitating collaborations, and making ECEI/MIR data products available to the widest possible user base.

An example of the FWR2D code in action is given in Figure 19 below. This synthetic diagnostic employs M3D-C1 output and details of the diagnostic antenna patterns taken from laboratory analysis is far characterization, models the plasma-wave interaction in 3D, and produces a synthetic time trace that may be processed in the same way as real data. Specifically, a saturated EHO mode structure is obtained in

M3D-C1. From this model, synthetic MIR signals are produced. They are analyzed to produce a poloidal wavenumber spectrum in the same manner as the real data from experiment, and a striking similarity

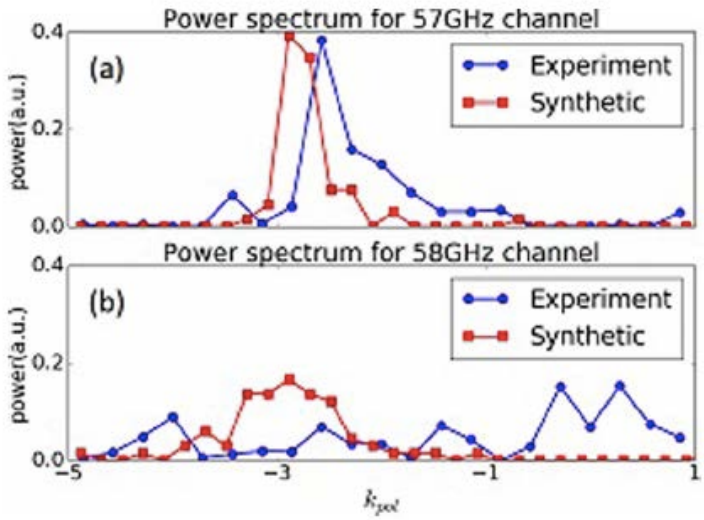

Figure 19. A comparison between MIR data and synthetic data obtained by applying synthetic diagnostics to M3D-C1 data. From L. Shi, et al., RSI 87, 11D303 (2016).

The FWR2D and 3D based synthetic diagnostic platform has been applied to both linear and non-linear modeling of the coherent EHO. The method of generating synthetic diagnostic signal from plasma simulation output is illustrated in Fig. 20. A time-series (or periodic sequence) of perturbed field data from simulation is combined with the optical field patterns of the diagnostic to produce time-dependent synthetic imaging data. Thousands of time-points can be generated thanks to the efficient algorithm of FWR3D, which utilizes a very efficient paraxial-wave solution to solve for propagation in regions far from the cutoff, but within the large (a/λ) plasma volume of DIII-D. These many frames of imaging data may be analyzed by the same methods applied to real data on DIII-D in order to understand the diagnostic response and features of the visualization. An example of synthetic images produced by the synthetic diagnostic is given in Fig. 21. The n=3 electron density fluctuation produced by M3D-C1 is shown at left. This perturbation is evolved in time to produce the images in the top row from an idealized MIR diagnostic with 6 probing frequencies (DIII-D MIR is currently equipped with 4 radial channels). The density data from M3D-C1 are plotted in the row of images underneath for comparison. Scaling the phase of the reflectometer signal (upper row) appropriately with the density perturbation (lower row), the two sequences are nearly indistinguishable. Note, however, that the phase of the MIR signal corresponds to radial fluctuation of the density cutoff layer, which also depends on the local gradient.

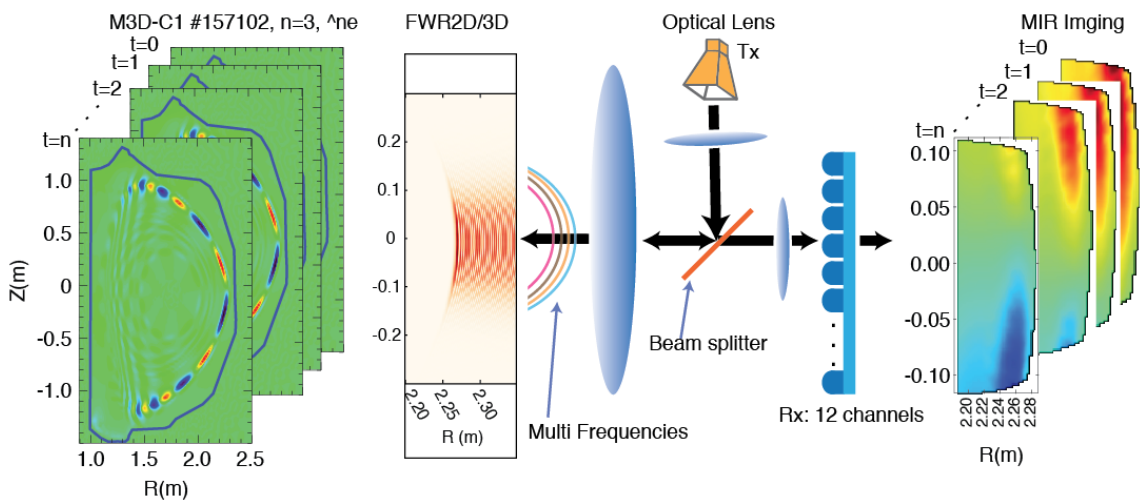

Figure. 20. The process of forward modeling MIR diagnostic output from 3D MHD plasma simulation. Time-dependent output from M3D-C1 has been provided for shot #157102 and n=3, 5 edge harmonic fluctuations. These are inserted as perturbed fields into the simulation domain of FWR3D. Antenna patterns taken from optical design, diffractive modeling, and laboratory characterization of the MIR imaging arrays are used as boundary conditions for the simulation. The converged electric field pattern at the outgoing microwave boundary is taken at each time step of the simulation and compared with the receiver antenna pattern to produce a quadrature (amplitude and phase) signal time-point. Thousands of time-points are combined to produce synthetic imaging data.

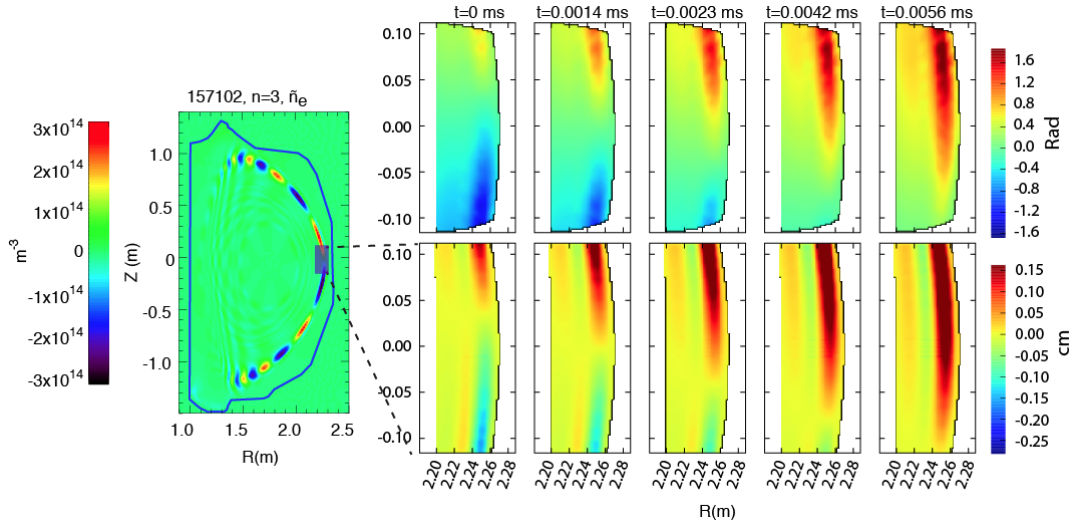

Figure 21. Modeled MIR measured mode structure (upper row) compared to mode structure from M3D-C1 (lower row) within the region accessible to MIR and at different time (toroidal position). The upper row shows the phase fluctuation from modeled MIR due to density fluctuation. The lower row shows the magnetic flux surface displacement from M3D-C1 simulations. The mode structure on upper row is measured accurately spatially and temporally.

Careful inspection of Microwave Imaging Reflectometer data from DIII-D has identified subtle features of the EHO mode structure, including a previously unrecognized inversion radius in the

fluctuating density response near the top of the QH-mode pedestal. This feature is often indicative of a magnetic island, and in our case represents a nonlinear modification of the eigenmode structure. Graduate students Xiaoxin Ren and Ming Chen of UC Davis, collaborating with Lei Shi (Princeton University) and Dr. Xi Chen (GA) have accomplished forward modeling of linear, time dependent M3D-C1 simulations for comparison with experiment. This work was reported at the 1st European Conference on Plasma Diagnostics in Frascati, Italy, and published in both the Journal of Instrumentation (JINST) and Proceedings of Science (PoS).

A major component of UC Davis graduate student Ming Chen's dissertation project concerned the physics of edge fluctuations that establish nonlinearly saturated, ELM free H-mode conditions on DIII-D. Specifically, she investigated the impact of aspects beyond linear, ideal MHD on the destabilization and regulation of the so-called coherent EHO by comparing progressively more sophisticated MHD simulations to microwave imaging data using the FWR synthetic diagnostic. Toroidal fluid flow and E×B shear have been identified as important elements of mode stability and nonlinear evolution. Flows modify the linear growth rates of various instabilities, and the ratio of linear growth rate to flow shear in turn modifies the mode structure. Changes in mode structure then modify transport, which provides feedback on the flow and flow shear. This nonlinear cycle leads either to a transient event, as is the case with an ELM crash, or to a stationary, saturated state, and imaging diagnostics are powerful tools for characterizing this behavior and identifying a valid physics model.

Ming Chen was engaged in the development of FWR2D and FWR3D forward modeling of plasma simulation through collaboration with PPPL and Princeton University researchers since qualifying for Ph.D. candidacy in 2014 through her successful dissertation defense in May, 2018 and made impressive technical innovations allowing fully time-dependent 3D simulations from M3D-C1 and other codes to be coupled with full-wave diagnostic modeling [c.f. Lei Shi HTPD 2016 abstract, Ming Chen HTPD 2018 abstract]. She has also collaborated extensively with Benjamin Tobias, Chris Muscatello, and Xiaoxin Ren in their analysis of MIR data from DIII-D and applied similar methods to synthetic data. These comparisons of modeling and experiment have contributed to multiple publications and have notably been key to investigations by Xi Chen of General Atomics [APS-DPP 2015]. Figure 22 (a) demonstrates agreement, within error bars, between measured and simulated poloidal wavenumber for the EHO on DIII-D. Building upon the above work, we can use Ming Chen's forward modeling and data analysis tools to compare the radial and poloidal structure of the so-called coherent EHO modeled using M3D-C1, JOREK, and perhaps NIMROD to previous and upcoming experiments. Unique and interesting features of the MIR diagnostic response have already been identified in experiment, and we anticipate unique insights will be gained by the success or failure of reproducing these features with further MHD modeling.

Ming Chen has presented a comparison of MIR data with M3D-C1 modeling at the Transport Task Force meeting in Denver, Colorado. In this presentation, she provided new analysis of linear, time dependent M3D-C1 simulations that include sheared toroidal flow and a sheared EHO mode structure. A short-term goal is to directly measure the phase variation shown in Figure 22 (b) using MIR and ECEI for an improved understanding of its relationship to plasma flow shear and the calculated linear growth rate of the instability. These results were shown at the 18th International Congress on Plasma Physics (ICPP 2016) Kaohsiung, Taiwan, where Ming Chen gave a contributed talk.

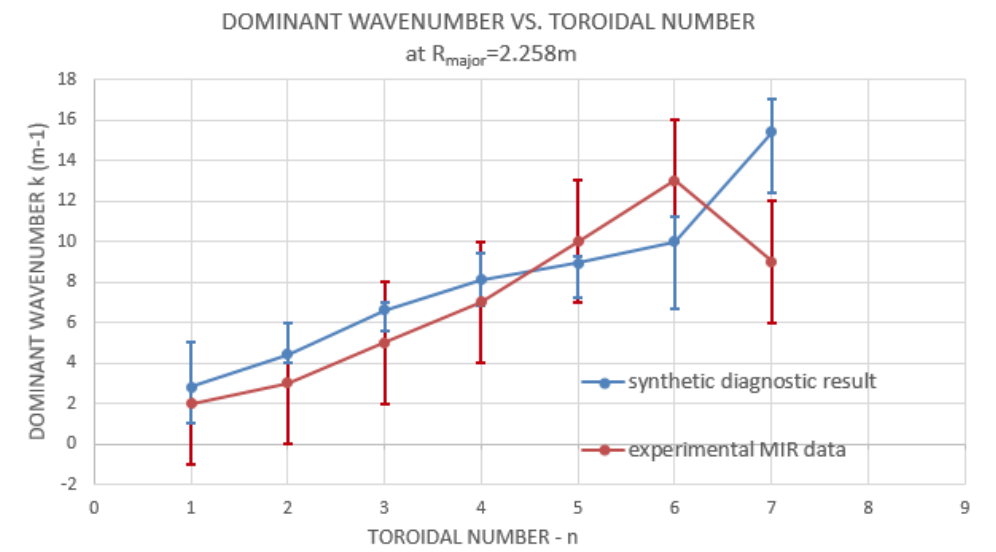

Figure 22 (a). Synthetic diagnostic forward modeling is applied to linear M3D-C1 modeling and compared with MIR data from DIII-D experiments. Within error bars, the poloidal wavenumber of the mode agrees with simulation for n-numbers 1-5.

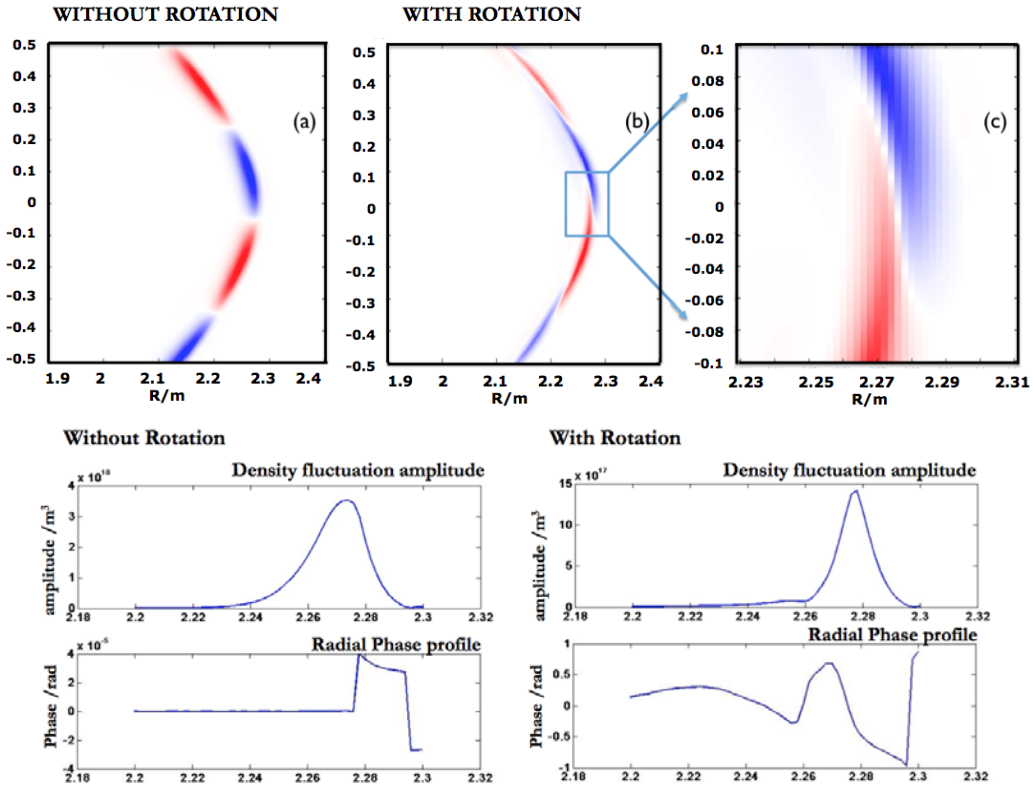

Figure 22 (b) M3D-C1 simulations with and without sheared toroidal flow generate very different mode structures. The sheared mode structure shown at right exhibits a phase shear that can be quantified and measured with MIR. Currently, synthetic diagnostic forward modeling is being performed so as to properly interpret and compare existing MIR data for these discharges.

Extending the full-wave synthetic reflectometer code FWR2D to include 3D effects was one important accomplishment of our recent collaborations with PPPL. Another major milestone has been the development of a synthetic ECEI diagnostic.

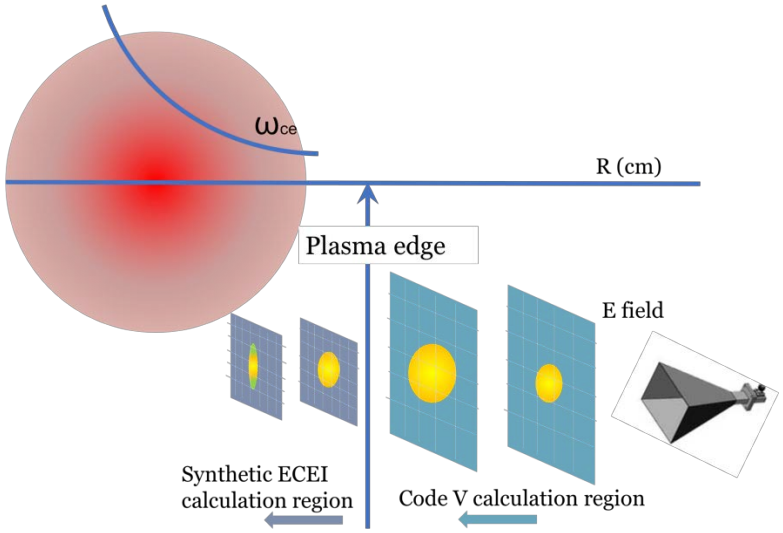

Figure 23 illustration of synthetic ECEI diagnostic with optical simulation integrated.

This synthetic ECE2D code employs an innovative reciprocal approach to relate the original incoherent emission problem to a coherent wave propagation and absorption calculation. The plasma emissivity, reabsorption, refraction, and diffraction effects on the ECE signals are all properly included. These effects become critically important when diagnosing edge plasmas. First, the pedestal is a region of finite and rapidly varying optical thickness where effects such as shine-through of down-shifted emission and competition with density fluctuations in optically grey regions become important. Second, conditions during the ELM are often close to density cutoff where refraction effects are important and change the mapping of ECEI channels. Third, the features of interest can be highly localized and comparable in size to the nominal resolution of a given ECEI channel. A simple demonstration of these multiple effects at play is given in Figure 24. The temperature and density are modeled as if well-behaved sinusoidal fluctuations with finite amplitudes and poloidal wavenumbers. The recorded ECE signal, however, is not sinusoidal. This is due to refraction which guides the radiation along channels of lower density, effectively shifting the viewing location in time with the propagation of the mode. Further analysis of the time trace in the frequency domain would show that the ECE signal is composed of multiple harmonics. However, this harmonic content is something of a diagnostic artifact; it is due to some feature of the mode, but does not directly reflect its structure. This is an excellent example of data that would easily be misinterpreted were it not for the ability to produce a high-quality forward model.

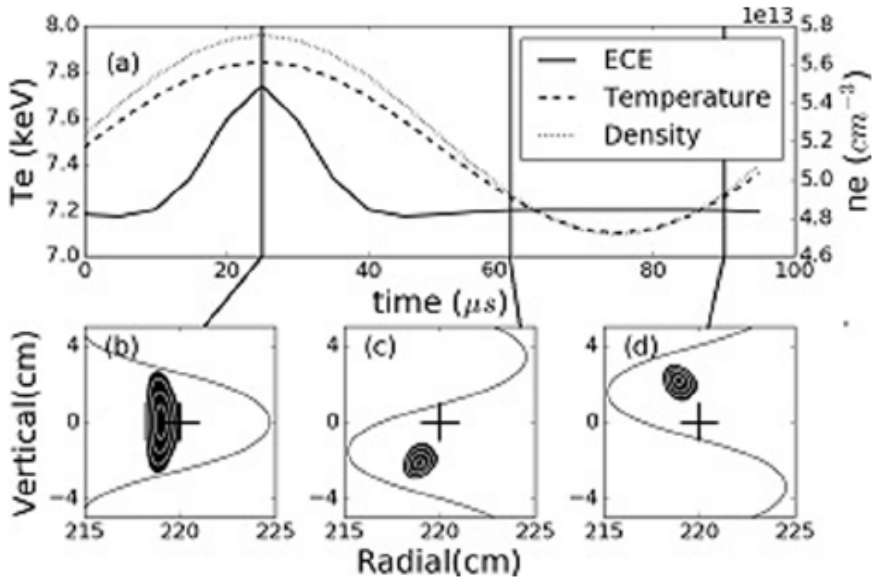

Figure 24. An illustration of refractive effects that impact ECEI diagnostics obtained by synthetic diagnostic modeling. The motion of the diagnosed detection region (emission spot) contributes to distortion of the diagnostic signal with respect to the local temperature fluctuation. From L. Shi, et al., RSI 87, 11D303 (2016).

With the confidence of the reliability of the 2D synthetic ECEI diagnostics obtained during extensive benchmarking tests, we applied it to compare the responses of the ECEI system under two optical designs: (1) conventional optics with no field curvature adjustment (FCA) lens and (2) with advanced FCA lens. The conventional imaging diagnostic system suffers from the commonly existing artifacts due to the field curvature in the optics design. This leads to aberrations in the image plane and strongly degrades the imaging performance. As for the case of the passive ECEI diagnostic system, since the frequency of the ECE signal is directly proportional to the local magnetic field strength which is monotonically decreasing along the major radius, the emission layer of the ECE signal is very close to a flat plane perpendicular to the major radius direction. However, in the traditional convex-lens-only optical designs, the image layer is inevitably curved (Figure 24). The mismatches between the flat emission layer and the curved image plane lead to the degradation of the image quality. When the two adjacent Gaussian beams are vertically aligned, the effect of crosstalk between them can be neglected and signals can still be well decoupled once the waist locations are shifted due to the field curvature, the crosstalk between these two signals will increase significantly, degrade the image performance, and lead to confusion in received signal interpretation. Thus, minimization of the field curvature artifact is one of the most important goals in the imaging optics design for tokamak plasma ECEI diagnostics.

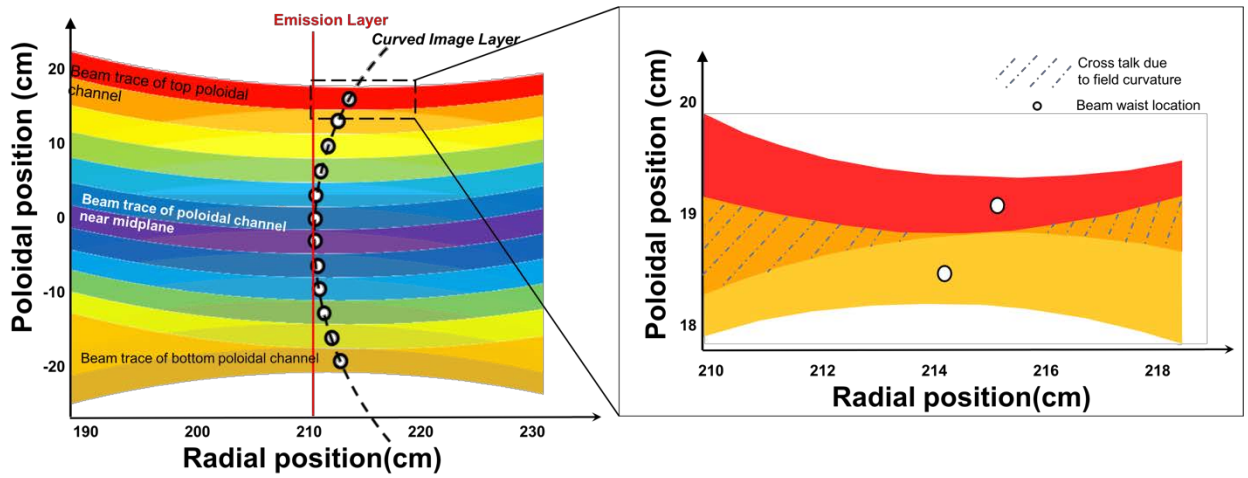

Figure 25. Curved image plane in the plasma region due to the field curvature presence in Gaussian beam framework. In the left figure, the dashed lines are the waist locations of the edge and center channels, and the solid black line is the curved image plane, and the dotted and dashed black line denotes one flat emission layer. The right figure is a schematic of the changes in the crosstalk between the adjacent channels when the field curvature is present. Here, the dots are the waist locations of the two channels, and the masked region with dash lines are the cross-talk region due to field curvature

In order to solve the field curvature problem as described above, an imaging optics design for the ECE imaging system on the EAST tokamak with the so-called Field Curvature Adjustment lens 26) was developed[Zhu, Y., et al., *The general optics structure of millimeter-wave imaging diagnostic on TOKAMAK*. Journal of Instrumentation, 2016. **11**(01): p. P01004.]. This permitted us to evaluate the improvement arising from the application of the Field Curvature Adjustment (FCA) lenses with the aid of the synthetic ECEI2D codes.

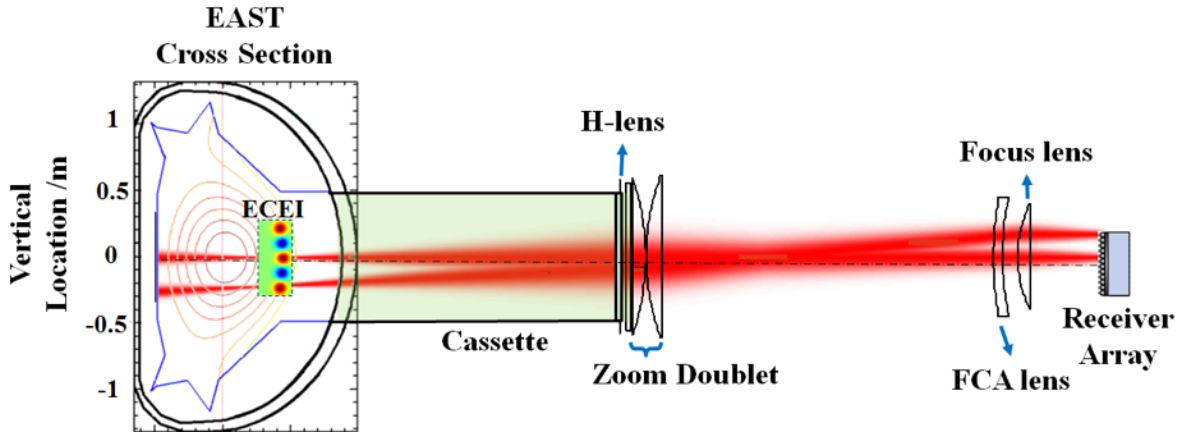

Figure 26. ***Gaussian beam trace results of the edge-most and center channels shown as the red beams; the black dashed line is the main axis of the optics. The ECEI observation region and the pre-defined poloidal mode structure are overlaid on the cross section of the EAST tokamak. In the EAST cross section part, the black and blue contour lines show the locations of the outer wall and inner wall, and the orange contour lines represent the flux surfaces where the eigenmodes locate.***

In the FCA-aided EAST ECEI system, there are a total of 16 (radial) × 24 (poloidal) = 384 channels. The focal plane is around 220 cm with a depth of focus of 16.9 cm. In the synthetic simulation, given the computational efficiency and for illustration purposes, we are only using 4 (radial) × 24 (poloidal) = 96 ECEI channels. The frequencies used are 90, 92, 94, and 96 GHz which covers the radial range from 208 cm to 222 cm and the poloidal range extends from around -20 cm to 20 cm. The locations of the EAST ECEI channels are overlaid on the filled Contour plot, shown as '+' . Since this ECEI system is for the EAST tokamak, the EAST related profile parameters are used: R = 185 cm, a = 45 cm. In order to avoid the situation where the injecting beam frequency falls in the optically thin region, the simulated magnetic field is set to B = 2.0 T.

As shown in a predefined eigenmode structure is present in the low field side of the cross section of the EAST tokamak with some background noise, and the equilibrium T_e profile is set to be uniformly distributed at 5 keV. The synthetic ECEI diagnostic is performed to compare the performance of the synthetic diagnosed results of the conventional non-FCA optical system design with those of the FCA design.

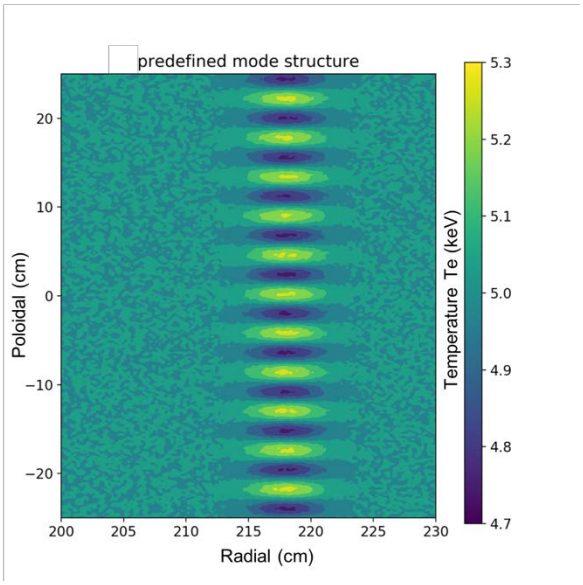

Figure 27. Predefined mode structure of temperature fluctuations with some random background noise.

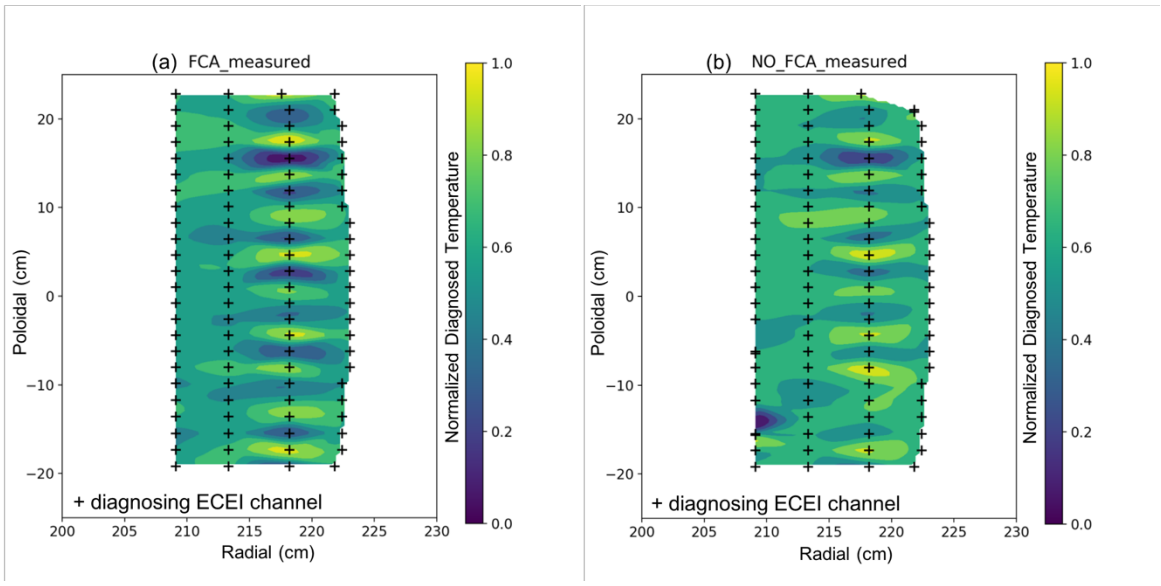

Figure 28 ***Synthetic diagnostic result (a) with FCA design: the synthetic diagnostic reproduces the predefined mode structure; (b) without FCA design: the synthetic diagnostic result is not reliable***.

When the poloidal wavenumber is small, both the non-FCA and FCA systems can well-diagnose the predefined structure. When approaching the resolution limit, the results are shown in: the mode structure as well as the measured temperature fluctuation diagnosed from the synthetic diagnostic result for the non-FCA case is quite different from the predefined structure, which is a result of the degraded performance due to field curvature. However, for the FCA case, the predefined fluctuations can still be well diagnosed. The synthetic ECEI diagnostic results show that, with FCA lenses applied, the upgraded ECEI system has significant advantages in focusing on high poloidal wavenumber structures with the aberrations from the spherical surfaces corrected. This result shows that FCA lenses are necessary in the design of next generation microwave imaging diagnostics to correct the image distortion due to the field curvature. Ming Chen presented these results at the 22nd Topical Conference on High-Temperature Plasma Diagnostics (HTPD 2018) and the related paper had been accepted by the Review of Scientific Instruments and is in the publish process.

Figure 29 provides details of the development path for a fully comprehensive Synthetic Diagnostics Platform (SDP), which continues, albeit at a much slower rate. This development effort will be shared by UC Davis researchers for whom we request funding under this proposal and independently funded collaborators at PPPL and UC Irvine. The SDP is built using open-source Python libraries and already includes sophisticated synthetic diagnostic modules for generating synthetic ECEI, MIR, BES, and Mirnov array data. It also includes modules for reading and processing simulation data from M3D-C1, XGC, GTS, and GTC. Modules to couple NIMROD, BOUT++, and JOREK are under development. Other key elements of this development plan include integration into the OMFIT environment at DIII-D where it will be coupled to kinetic equilibrium/transport reconstruction (kEFIT/TRANSP) the full suite of ECEI and MIR visualization routines. The roadmap follows below.

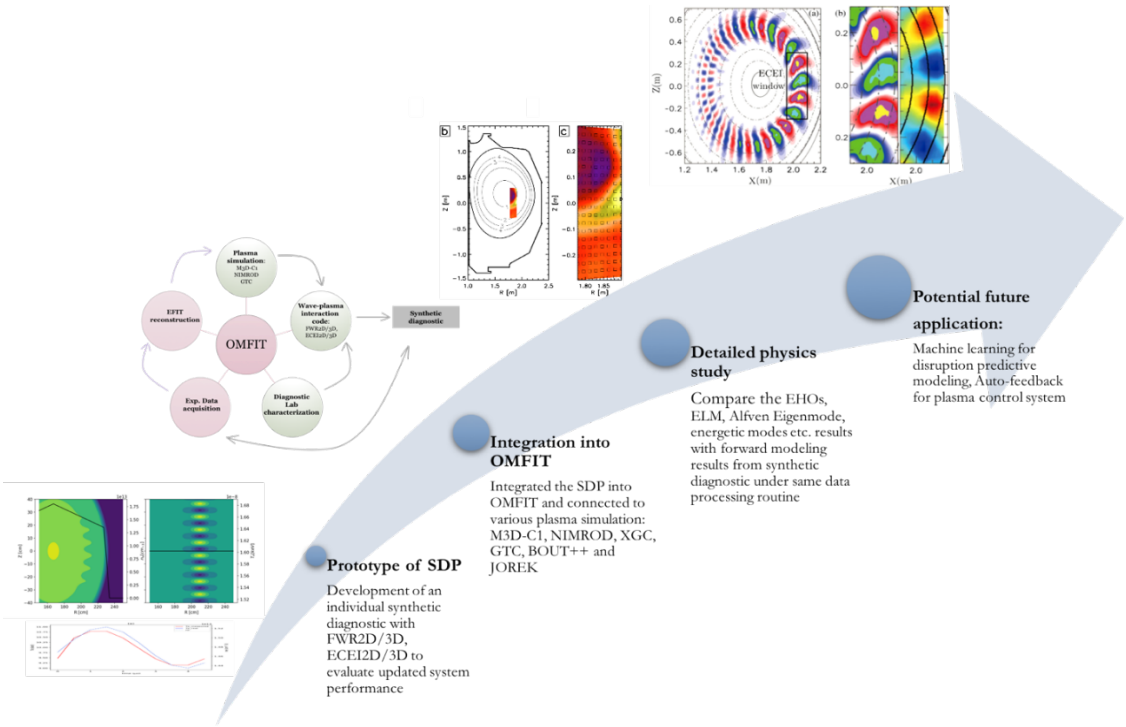

Figure 29. Roadmap for synthetic diagnostic development

Product Details

Journal Papers

A.Mase, Y. Kogi, D. Kuwahara, Y.Nagayama, N. Ito, T. Maruyama, H. Ikezi, X. Wang, M. Inutake, T. Tokuzawa, J. Kohagura, M. Yoshikawa, S. Shinohara, B.J. Tobias, C. Muscatello, X. Ren, M. Chen, C.W. Domier, N.C. Luhmann, Jr., "Development and Application of Radar Reflectometer Using Micro- to Infrared Waves," Advances in Physics: X (TAPX), 3 (1), 1472529, 2018.

Y. Wang, B. Tobias, Y.-T. Chang, J.-H. Yu, M. Li, F. Hu, M. Chen, M. Mamidanna, T. Phan, A.-V. Pham, J. Gu, X. Liu, Y. Zhu, C.W. Domier, L. Shi, E. Valeo, G.J. Kramer, D. Kuwahara, Y. Nagayama, A. Mase, and N.C. Luhmann Jr., "Millimeter-wave imaging of magnetic fusion plasmas: technology innovations advancing physics understanding," *Nuclear Fusion*, **57** (7), 072007, 2017.

Xi Chen, K.H. Burrell, N.M. Ferraro, T.H. Osborne, M.E. Austin, A.M. Garofalo, R.J. Groebner, G.J. Kramer, N.C. Luhmann Jr, G.R. McKee, C.M. Muscatello, R. Nazikian, X. Ren, P.B. Snyder, W.M. Solomon, B.J. Tobias and Z. Yan, "Rotational shear effects on edge harmonic oscillations in DIII-D quiescent H-mode discharges," *Nuclear Fusion*, **56** (7), 076011, 2016.

B. Tobias, C. W. Domier, N. C. Luhmann Jr., C. Luo, M. Mamidanna, T. Phan, A.-V. Pham and Y. Wang, "Low-noise heterodyne receiver for electron cyclotron emission imaging and microwave imaging reflectometry," *Review of Scientific Instruments*, **87** (11) 11E103, 2016.

B. Tobias, M. Chen, I. G. J. Classen, C. W. Domier, R. Fitzpatrick, B. A. Grierson, N. C. Luhmann Jr., C. M. Muscatello, M. Okabayashi, K. E. J. Olofsson and C. Paz-Soldan, "Rotation profile flattening and toroidal flow shear reversal due to the coupling of magnetic islands in tokamaks," **(Invited),** *Physics of Plasmas*, **23** (5), 056107, 2016.

Y. L. Zhu, J. L. Xie, C. X. Yu, Z. L. Zhao, B. X. Gao, D. X. Chen, W. D. Liu,W. Liao, C. M. Qu, C. Luo, X. Hu, A. G. Spear, N. C. Luhmann Jr., C. W. Domier, M. Chen, X. Ren and B. J. Tobias, "Millimeter-wave imaging diagnostics systems on the EAST tokamak," **(Invited),** *Review of Scientific Instruments*, **87** (11) 11D901, 2016.

X. Chen, K.H. Burell, T.H. Osborne, W.M. Solomon, K. Barada, A.M. Garofalo, R.J. Groebner, N.C. Luhmann, Jr., G.R. McKee, C.M. Muscatello, M. Ono, C.C. Petty, M. Porkolab, T.L. Rhodes, J.C. Rost, P.B. Snyder, G.M. Staebler, "Stationary QH-mode plasmas with high and wide pedestal at low rotation on DIII-D," *Nuclear Fusion*, **57** (2), 022007, 2016.

W. Shen, G. Fu, B. Tobias, M.A. Van Zeeland, F. Wang, and Z.-M. Sheng, "Nonlinear hybrid simulation of internal kink with beam ion effects in DIII-D," *Physics of Plasmas*, **55**(7) 073001, 2015.

M. Kim, J. Lee, H.K. Park, G.S. Yun, W. Lee, C.W. Domier, N.C. Luhmann, Jr., KSTAR team, "Multimode excitation during the inter-elmcrash periods in KSTAR H-mode plasma," *Nuclear Fusion, **55**(7) 073001, 2015.*

X. Ren, M. Chen, X. Chen, C.W. Domier, N.M. Ferraro, G.J. Kramer, N.C, Luhmann, Jr., C.M. Muscatello, R. Nazikian, L. Shi, B.J. Tobias, and E. Valeo, "Microwave Imaging Reflectometry for the study of Edge Harmonic Oscillations on DIII-D," *ECPD JINST special issue*, **10** (10) 10036, 2015.

S. E. Zemedkun, S. Che, Y. Chen, C. W. Domier, N. C. Luhmann Jr., T. Munsat,S. E. Parker, B. Tobias, W. Wan andL. Yu, "Spatially resolved measurements of two-dimensional turbulent structures in DIII-D plasmas," *Physics of Plasmas*, **22** (12) 122508, 2015.

Y. Zhu, J. Xie, W.D. Liu, C. Luo, Z. Zhao, D. Chen, C.W. Domier, N.C. Luhmann, Jr., M. Chen, X. Hu, "The general optics structure of millimeter-wave imaging diagnostic on tokamak," *Journal of Instrumentation*, **11** (1), 01004, 2015.

D. Eldon, R. L. Boivin, C. Chrystal, R. J. Groebner, G. R. McKee, L. Schmitz, G. R. Tynan, Z. Yan, J. A. Boedo, K. H. Burrell, J. D. King, E. Kolemen, N. C. Luhmann Jr., C. M. Muscatello, T. H. Osborne and

P. B. Snyder, "Evolution of E × B shear and coherent fluctuations prior to H-L transitions in DIII-D and control strategies for H-L transitions," *Physics of Plasmas*, **22**, 112506, 2015.

Conference Paper/Presentation

M. Chen, Y. Zhu, C. Luo, L. Shi, B.J. Tobias and N. C. Luhmann, Jr., "Synthetic Diagnostic for Electron Cyclotron Emission Imaging," High Temperature Plasma Diagnostics, San Diego, California 04/16/2018.

J.-H. Yu, Y.-T. Chang, K.-Y. Lin, C-C. Chang, S.-F. Chang, Y. Ye, A.V. Pham, B.J. Tobias, Y. Zhu, C.W. Domier and N.C. Luhmann, Jr., "Millimeter-wave system-on-chip advancement for fusion plasma diagnostics," High Temperature Plasma Diagnostics, San Diego, California 04/16/2018.

Y. Zhu, Y. Ye, J-H. Yu, B. Tobias, A-V Pham, Y. Wang, C. Luo, C.W. Domier, G. Kramer, Y. Ren, A. Diallo, R. Nazikian, M. Chen, G. Yu, N.C. Luhmann, Jr., "Liquid Crystal Polymer Receiver Modules for Electron Cyclotron Emission Imaging on the DIII-D Tokamak," High Temperature Plasma Diagnostics, San Diego, California 04/16/2018.

Y. Zhu, Y. Wang, B. Tobias, J.-H. Yu, A.-V. Pham, C.W. Domier, C. Luo, A. Diallo, G. Kramer, Y. Ren, R. Nazikian,M. Chen and N. Luhmann, Jr., "ECE Imaging upgrade for ELM imaging measurement on DIII-D," 59th Annual Meeting of the APS Division of Plasma Physics, Milwaukee, Wisconsin, 10/23/2017.

Ming Chen, B.J. Tobias, A. Diallo, K. Burrell, G.R. Mckee, Z. Yan, G.J. Kramer, Y. Ren, C. Luo, Y. Zhu, and N.C. Luhmann, Jr., "Experimental observation from DIII-D of the effect of E×B shear on EHO's structure and edge transport," 1st Asia-Pacific Conference on Plasma Physics (AAPPS-DPP2017), Chengdu, China, 09/18/2017.

Y. Zhu, Y. Wang, B. Tobias, C. Luo, J.-H. Yu, A.-V. Pham, C.W. Domier, A. Diallo, G.J. Kramer, Y. Ren, R. Nazikian, and N.C. Luhmann, Jr., "System-on-Chip (SoC) Technology for Tokamak Electron Cyclotron Emission Imaging and Microwave Imaging Reflectometry," 1st Asia-Pacific Conference on Plasma Physics (AAPPS- DPP2017), Chengdu, China, 09/18/2017.

Fengqi Hu, Meijiao Li, Calvin W. Domier, Xiaoguang Liu, Neville C. Luhmann, Jr., "Microwave imaging radar reflectometer system utilizing digital beam forming," 58th Annual Meeting of the APS Division of Plasma Physics, San Jose, CA, 10/31/2016.

Tobias, B., N. Ferraro, S. Jardin, G. Kramer, T. Evans, C. W. Domier, and N. C. Luhmann Jr., "Correlated enhancement of momentum and stochastic energetic ion transport due to multi-helicity tearing modes on DIII-D," 58th Annual Meeting of the APS Division of Plasma Physics, San Jose, CA, 10/31/2016.

Muscatello, C. M., K. H. Burrell, N. C. Luhmann Jr, G. R. McKee, and B. Tobias, "Characterization of broadband fluctuations in wide-pedestal QH-mode plasmas on DIII-D," 58th Annual Meeting of the APS Division of Plasma Physics, San Jose, CA, 10/31/2016.

Lee, Jaehyun, Gunsu Yun, Minjun Choi, Jae-Min Kwon, Young-Mu Jeon, Woochang Lee, Neville C. Luhmann Jr, and Hyeon K. Park, "Nonlinear interaction between edge-localized modes (ELMs) and edge turbulence during ELM-crash-suppression phase under n= 1 RMP," 58th Annual Meeting of the APS Division of Plasma Physics, San Jose, CA, 10/31/2016.

Yang Wang, "Low-noise superheterodyne receiver array for ECEI and MIR," 58th Annual Meeting of the APS Division of Plasma Physics, San Jose, CA, 10/31/2016.

Xing Hu, A.G. Spear, Yilun Zhu, C.W. Domier, Jinlin Xie, N.C. Luhmann, Jr., "Development of the Microwave Imaging Reflectometer (MIR) for the EAST Tokamak," 18th International Congress on Plasma Physics ICPP 2016, Kaohsiung, Taiwan, 06/29/2016.

N.C.Luhmann, Jr., Yu-Ting Chang, Ming Chen, I. Classena, C.W. Domier, J. Gu, Fengqi Hu, Xing Hu, M. Jiang, G.J. Kramer, D. Kuwahara, Meijiao Li, X. Liu, M. Mamidann, A. Mase, C. M. Muscatello, A.-V. Pham, T. Phan, Xiaoxin Ren, L. Shi, A.G. Spear, B. Tobias, E. Valeo, B. Vanovac,Y. Wang, Jo-Han

Yu, Yilun Zhu, "Millimeter-Wave Imaging of Magnetic Fusion Plasmas: Technology Innovations Advancing Physics Understanding," 18th International Congress on Plasma Physics ICPP 2016, Kaohsiung, Taiwan, 06/29/2016.

L. Shi, E. J. Valeo, B. J. Tobias, G. J. Kramer. Hausammann,W. M. Tang, M. Chen, "Fusion Plasma Synthetic Diagnostics Platform," Proceedings of the 21st Topical Conference on High- Temperature Plasma Diagnostics, Madison, Wisconsin, 06/06/2016.

Y. L. Zhu, J. L. Xie, C. X. Yu, Z. L. Zhao, B. X. Gao, D. X. Chen, W. D. Liu, W. Liao, C. M. Qu, C. Luo, X. Hu, A. G. Spear, N. C. Luhmann Jr., C. W. Domier, M. Chen, X. Ren and B. J. Tobias, "Millimeter-wave imaging diagnostics systems on EAST Tokamak," **(Invited),** Proceedings of the 21st Topical Conference on High- Temperature Plasma Diagnostics, Madison, Wisconsin, 06/06/2016.

B. Tobias, C. W. Domier, N. C. Luhmann Jr., C. Luo, M. Mamidanna, T. Phan, A.-V. Pham and Y. Wang, "Low-noise GaAs and Liquid Crystal Polymer heterodyning receiver circuits for ECE- Imaging and Microwave Imaging Reflectometry," Proceedings of the 21st Topical Conference on High-Temperature Plasma Diagnostics, Madison, Wisconsin, 06/06/2016.

Ming Chen, X. Ren, N. C. Luhmann, Jr., B. J. Tobias, L. Shi, G.J.Kramer , C.M.Muscatello , X.Chen , A. M. Garafalo, F.Liu , G.Huijsmans, "Forward Modeling of Microwave Imaging Reflectometry for the Study of Edge Harmonic Oscillations in Quiescent H-Mode," 2016 US Transport Task Force Workshop, Denver, Colorado, 03/29/2016.

L. Shi, G. Kramer, W. Tang, B. Tobias, E. Valeo, R. Churchill, L. Hausammann, "Recent Progress and Future Plans for Fusion Plasma Synthetic Diagnostics Platform," 57th Annual Meeting of the APS Division of Plasma Physics, Savannah, Georgia, 11/16/2015.

Hannah Hoffmann, B.J. Tobias, "2D Imaging of ELM Structures Using Microwave Imaging Reflectometry," 57th Annual Meeting of the APS Division of Plasma Physics, Savannah, Georgia, 11/16/2015.

C.M. Muscatello, K.H. Burrell, Xi Chen, N.C. Luhmann, Jr., B.A. Grierson, G.J. Kramer, B.J. Tobias, "Disparate-scale coupling of turbulence in QH-mode plasmas on DIII-D," 57th Annual Meeting of the APS Division of Plasma Physics, Savannah, Georgia, 11/16/2015.

Jaehyun Lee, Minjun Choi, Gunsu Yun, Woochang Lee, Hyeon K. Park, Neville C. Luhmann, Jr., "Observation of edge turbulence spread by ECEI on the ELM- crash-suppressed plasmas in the KSTAR," 57th Annual Meeting of the APS Division of Plasma Physics, Savannah, Georgia, 11/16/2015.

B.J. Tobias, "Collapse of core toroidal angular momentum due to the coupling of rotating magnetic islands in tokamaks," 57th Annual Meeting of the APS Division of Plasma Physics, Savannah, Georgia, 11/16/2015.

Xi Chen, K.H. Burrell, N. M. Ferraro, T.H. Osborne, M.E. Austin, A.M. Garofalo, R.J. Groebner, G.J. Kramer, N.C. Luhmann Jr., G.R. Mckee, C.M. Muscatello, R. Nazikian, X. Ren, P.B. Snyder, "Rotational Shear Effects on Edge Harmonic Oscillations in DIIID Quiescent H-mode Discharges," 57th Annual Meeting of the APS Division of Plasma Physics, Savannah, Georgia, 11/16/2015.

N.C. Luhmann, Jr., Yu-Ting Chang, Ming Chen, Xi Chen, C.W. Domier, J. Gu, Fengqi Hu, Xing Hu, G.J. Kramer, Meijiao Li, X. Liu, M. Mamidanna, A.-V. Pham, T. Phan, Xiaoxin Ren, L. Shi, A.G. Spear, B. Tobias, Yilun Zhu, "Advances in 2-D Millimeter-Wave Plasma Imaging of Magnetic Fusion Plasmas," 25th International Toki Conference, Ceratopia Toki, Toki-city, Gifu, JAPAN, 11/03/2015.

Y. Zhu, J. Xie, W.D. Liu, C. Luo, Z. Zhao, D. Chen, C.W. Domier, N.C. Luhmann Jr., M. Chen and X. Hu, "The general optics structure of millimeter-wave imaging diagnostic on TOKAMAK," 17th International Symposium on Laser-Aided Plasma Diagnostics, Sapporo, Hokkaido, Japan, 09/27/15

Xing Hu; Calvin Domier; Neville Luhmann, Jr., "Frequency Selective Surface Applications In Millimeter Wave Imaging Diagnostics For Fusion Plasmas," 2015 40th International Conference on Infrared, Millimeter, and Terahertz waves (IRMMW-THz), Hong Kong, 08/24/2015.

M. Li, C. Domier, X. Liu, N. C. Luhmann, Jr., “Wide band MM-wave, double-sided printed bow-tie antenna for phased array applications,” Proceeding of 2015 IEEE International Symposium on Antennas and Propagation,Vancouver, Canada, 07/19/2015.

Xi Chen, K.H. Burrell, N.M. Ferraro, T.H. Osborne, C.M. Muscatello, C.C. Petty, A.M. Garofalo, P.B. Snyder, R.J. Groebner, R. Nazikian, G.J. Kramer, B.J. Tobias, W.M. Solomon, Z. Yan, G.R. McKee, X. Ren, N.C. Luhmann Jr., and M.E. Austin, “Understanding The Physics Of Eho In Qh-Mode On Diii-D Including The Role Of Rotation Shear,” 42nd EPS Conference on Plasma Physics, Lisbon, Portugal, 06/22/2015.

B. Tobias, G.J. Kramer, and E. Valeo, C.M. Muscatello, X. Ren, M. Chen, A.G. Spear, A.V. Pham, T. Phan, M. Mamidanna, J. Lai, M. Li, D. Fu, F. Hu, C.W. Domier, and N.C. Luhmann, Jr., X. Chen, N. Ferraro, A. Garofalo, S. Zemedkun and T.L. Munsat, Y. Zhu, “Microwave Imaging Reflectometry (Mir) On The Diii-D Tokamak,” 1st EPS Conference on Plasma Diagnostics (ECPD), Frascati, Italy, 04/14/2015.

Xi Chen, K.H. Burrell, N.M. Ferraro, T.H. Osborne, C.M. Muscatello, C.C. Petty, A.M. Garofalo, P.B. Snyder, R.J. Groebner, R. Nazikian, G.J. Kramer, B.J.Tobias, W.M. Solomon, Z. Yan, G.R. McKee, X. Ren, N.C. Luhmann Jr., and M.E. Austin, “Understanding the Physics of EHO in QH-MODE on DIII-D Including the Role of Rotation Shear,” 1st EPS Conference on Plasma Diagnostics (ECPD), Frascati, Italy, 04/14/2015.

B. Tobias, I.G.J. Kramer, R. Nazikian, L. Shi, E. Valeo, M. Chen, C.W. Domier, N.C. Luhmann, Jr., T.L. Munsat, C.M. Muscatello, X. Ren and S. Zemedkun, “Microwave Imaging Reflectometry on DIII-D,” 1st EPS Conference on Plasma Diagnostics (ECPD), Frascati, Italy, 04/14/2015.

B. Tobias, G.J. Kramer, E. Valeo, C.M. Muscatello, X. Ren, M. Chen, A.G. Spear, A.V. Pham, T. Phan, M. Mamidanna, J. Lai, M. Li, D. Fu, F. Hu, C.W. Domier, N.C. Luhmann, Jr. X. Chen, N. Ferraro, A. Garofalo, S. Zemedkun, T.L. Munsat, Y. Zhu, “Microwave imaging reflectometry (MIR) on the DIII-D tokamak,” Proceedings of Science ECPD2015, Rome, Italy, 04/14/2015.

S.E. Zemedkun, Y. Chen, Jr, T. Munsat, S.E. Parker, W. Wan, S. Che, C.W. Domier, N.C. Luhmann, L. Yu, B.J. Tobias, “Microwave Imaging Reflectometry on DIII-D,” Proceedings of Science ECPD2015, Rome, Italy, 10/13/2014.

G. R. McKee, C. Holland, Z. Yan, E. J. Doyle, T. C. Luce, A. Marinoni, C. C. Petty, T. Rhodes, L. Schmitz, W. M. Solomon, B. J. Tobias, G. Wang, and L. Zeng, “Turbulence Behavior and Transport Response Approaching Burning Plasma Relevant Parameters,” Proceedings of the 25th International Conference on Fusion Energy, St. Petersburg, Russia, 10/13/2014.